

Pyridoxine-Dependent Epilepsy in Zebrafish Caused by *Aldh7a1* Deficiency

Izabella A. Pena,^{*,†,‡,1} Yann Roussel,^{*} Kate Daniel,^{*} Kevin Mongeon,^{*,†} Devon Johnstone,^{*,†}
Hellen Weinschutz Mendes,[‡] Marjolein Bosma,[§] Vishal Saxena,[‡] Nathalie Lepage,^{*} Pranesh Chakraborty,^{*}
David A. Dymant,^{*,†} Clara D. M. van Karnebeek,^{§,***} Nanda Verhoeven-Duif,^{††} Tuan Vu Bui,^{*}
Kym M. Boycott,^{*,†} Marc Ekker,^{*,2} and Alex MacKenzie^{*,†,2}

^{*}Children's Hospital of Eastern Ontario Research Institute and [†]Department of Pediatrics, Faculty of Medicine, University of Ottawa, Ontario K1H 8L1, Canada, [‡]Department of Biology, University of Ottawa, Ontario K1N 6N5, Canada, [§]Departments of Pediatrics and Clinical Genetics, Academic Medical Centre, 1105 AZ Amsterdam, The Netherlands, ^{***}Department of Pediatrics, Centre for Molecular Medicine and Therapeutics, University of British Columbia, Vancouver V5Z 4H4, British Columbia, Canada, and ^{††}Department of Genetics, Center for Molecular Medicine, University Medical Center (UMC), 3584 EA Utrecht, The Netherlands

ORCID IDs: 0000-0001-5242-3724 (I.A.P.); 0000-0003-3352-5631 (C.D.M.v.K.); 0000-0003-0024-1544 (T.V.B.); 0000-0003-4186-8052 (K.M.B.)

ABSTRACT Pyridoxine-dependent epilepsy (PDE) is a rare disease characterized by mutations in the lysine degradation gene *ALDH7A1* leading to recurrent neonatal seizures, which are uniquely alleviated by high doses of pyridoxine or pyridoxal 5'-phosphate (vitamin B6 vitamers). Despite treatment, neurodevelopmental disabilities are still observed in most PDE patients underlining the need for adjunct therapies. Over 60 years after the initial description of PDE, we report the first animal model for this disease: an *aldh7a1*-null zebrafish (*Danio rerio*) displaying deficient lysine metabolism and spontaneous and recurrent seizures in the larval stage (10 days postfertilization). Epileptiform electrographic activity was observed uniquely in mutants as a series of population bursts in tectal recordings. Remarkably, as is the case in human PDE, the seizures show an almost immediate sensitivity to pyridoxine and pyridoxal 5'-phosphate, with a resulting extension of the life span. Lysine supplementation aggravates the phenotype, inducing earlier seizure onset and death. By using mass spectrometry techniques, we further explored the metabolic effect of *aldh7a1* knockout. Impaired lysine degradation with accumulation of PDE biomarkers, B6 deficiency, and low γ -aminobutyric acid levels were observed in the *aldh7a1*^{-/-} larvae, which may play a significant role in the seizure phenotype and PDE pathogenesis. This novel model provides valuable insights into PDE pathophysiology; further research may offer new opportunities for drug discovery to control seizure activity and improve neurodevelopmental outcomes for PDE.

KEYWORDS pyridoxine-dependent epilepsy; *aldh7a1*; zebrafish model; lysine metabolism; metabolic epilepsy

PYRIDOXINE-DEPENDENT epilepsy (PDE, MIM #266100) is a rare autosomal recessively inherited metabolic disease (Gospe 2017) in which intractable and recurrent neonatal or infantile seizures are alleviated uniquely by high doses of pyridoxine (Pyr, vitamin B6) or pyridoxal 5'-phosphate (PLP)

(Baxter 2001; Mills *et al.* 2006; Stockler *et al.* 2011). When untreated, PDE can lead to death, usually of status epilepticus (Gospe 2017). This condition is caused by mutations in the lysine degradation gene *ALDH7A1* (Mills *et al.* 2006) that encodes α -amino adipic semialdehyde dehydrogenase, which is also known as "Antiquitin" (Lee *et al.* 1994) due to its remarkable level of conservation through evolution (Supplemental Material, Figure S1). Loss of *ALDH7A1* enzyme function leads to the pathogenic accumulation of the lysine intermediates amino adipate semialdehyde (AASA) and its cyclic equilibrium form piperidine 6-carboxylate (P6C) in tissues including the central nervous system (CNS) [4] (Figure 1). P6C has been shown to react with and inactivate PLP (the active form of vitamin B6), a cofactor for over 140 enzymes including those

Copyright © 2017 by the Genetics Society of America

doi: <https://doi.org/10.1534/genetics.117.300137>

Manuscript received August 11, 2017; accepted for publication October 4, 2017; published Early Online October 10, 2017.

Available freely online through the author-supported open access option.

Supplemental material is available online at www.genetics.org/lookup/suppl/doi:10.1534/genetics.117.300137/-/DC1.

¹Corresponding author: Children's Hospital of Eastern Ontario Research Institute, University of Ottawa, 401 Smyth Rd., Ottawa, ON K1H 8L1, Canada. E-mail: ipena2@uottawa.ca

²These authors contributed equally to this work.

involved in neurotransmission (Percudani and Peracchi 2003). It is thus hypothesized that the local or global depletion of PLP results in the Pyr-dependent seizures (Clayton 2006), possibly via disturbance of the PLP-dependent biosynthesis of γ -aminobutyric acid (GABA), the main cerebral inhibitory neurotransmitter. So far, clinical data from cerebrospinal fluid (CSF) measurements of these compounds were inconclusive and the pathophysiology of PDE remains to be fully elucidated.

While PDE seizures are responsive to pharmacological dosages of Pyr, lifelong supplementation fails to prevent the neurodevelopmental disabilities observed in > 75% of PDE patients (Baxter 2001; Stockler *et al.* 2011; van Karnebeek *et al.* 2016). These include mild to severe developmental and cognitive disabilities including disorders of expressive language (van Karnebeek *et al.* 2016). This observation underscores the need for further studies on the pathophysiology of PDE and the development of novel therapies. Consequently, in addition to Pyr, adjunct treatment strategies of lysine restriction (van Karnebeek *et al.* 2012) and arginine supplementation (Mercimek-Mahmutoglu *et al.* 2014), separately or in combination [“triple therapy” (Coughlin *et al.* 2015)], have been recently introduced as attempts to both improve seizure control and moderate the long-term neurodevelopmental impact of PDE [for reviews see Pena *et al.* (2016), van Karnebeek *et al.* (2016), and Gospe (2017)].

Although the PDE disease gene has been known for more than a decade (Mills *et al.* 2006), there has been a dearth of genetically engineered animals modeling the disease. Zebrafish (*Danio rerio*) is a simple vertebrate species easily amenable to genetic manipulation, which has emerged as a successful model in epilepsy research (Baraban *et al.* 2005, 2013; Hortopan *et al.* 2010; Teng *et al.* 2011; Grone *et al.* 2016; Sourbron *et al.* 2016; Griffin *et al.* 2017). Here, we report the use of clustered regularly interspaced short palindromic repeat (CRISPR)/Cas9 gene editing to generate an *aldh7a1*-null zebrafish model that recapitulates the clinical and biochemical features of PDE. *Aldh7a1* loss-of-function led to the accumulation of the toxic PDE biomarkers, spontaneous, recurrent seizures from 10 days postfertilization (dpf), and premature death (by 14 dpf). As with PDE, Pyr or PLP treatment halts zebrafish seizures; moreover, it also prolongs the survival of the mutant fish. Mass spectrometry (MS) studies of untreated fish identified several alterations in amino acid levels, most remarkably in the lysine metabolism pathway. Importantly, low B6 vitamers and GABA levels were observed, which may suggest that PDE is, at least in part, a disorder of GABA homeostasis.

Materials and Methods

Zebrafish maintenance

Adult wild-type (WT) zebrafish were maintained according to standard procedures (Westerfield 2000). All experiments were carried out in accordance with animal care guidelines provided by the Canadian Council on Animal Care and the University of Ottawa animal care committees approved this study under the

protocol number BL-2678. The zebrafish room was maintained on a 14 hr light: 10 hr dark cycle, with lights-on at 9:00 AM and lights-off at 11:00 PM. Fish system water conditions were maintained in the following ranges by automated feedback controls: 29–30°, pH 7.5–8.0, and conductivity (EC) 690–710. Embryos were bleached 24 hr postfertilization. Zebrafish embryos and larvae were raised in plastic petri dishes (10-cm diameter) in an incubator maintained at 28.5° until 7 dpf in E3 embryo media. Their housing density was limited to a maximum of 60 individuals per dish until 6 dpf, when the larvae were split in groups of 20 or fewer individuals in 750 ml static tanks containing rotifer solution in 200 ml system water. Rotifers (*Brachionus plicatilis*) were obtained from Reed Mariculture and were fed RGComplete (APBreed). Larvae were fed with ~15 mg of Gemma 75 per day and 50 ml of fresh water was added every day. Food quantity was gradually increased as the larvae grew. Juveniles and adults were grown in 3-liter tanks and fed on Gemma 150 and Gemma 300, respectively. Survival experiments were performed usually with a minimum of five or six fish per experimental group. Pyr and PLP (Sigma [Sigma Chemical, St. Louis, MO]) was dissolved in the system water; larvae were exposed to treatment for 30 min daily. Lysine treatment was performed with 48 hr of exposure. We considered our replicates as biological replicates as each sample was a different individual larva.

Morpholino gene knockdown in zebrafish

Translation-blocking (TB) or splice-blocking (SB) morpholino oligonucleotides (MO) (Gene Tools, LLC, Philomath, OR) were diluted in H₂O to 1 mM stock solution. The working solution was prepared in 1× *Danio* Buffer for the microinjections in embryos at the single-cell stage. The TB morpholino sequence was obtained from Babcock *et al.* (2014) 5'-TCGGACACTCGGCAACAGTTTATGC-3' (referred in their paper as “*aldh7a1*-MO1”), targeting the first coding exon of the zebrafish gene. We used injections of 7.5 ng of MO to replicate the procedure described in Babcock *et al.* (2014) as well as testing a lower dose (3.5 ng). The control MO (5'-CCTCTTACCTCAGTTACAATTTATA-3') and SB morpholino designed to target the intron 4–exon 5 splice junction “*aldh7a1*-SBMO-1” (5-GACACCTACGCATAGCAAACCTCTG-3') were also obtained from Gene Tools, and 2.5 ng was similarly injected at the single-cell stage.

Western blot

Total soluble proteins were extracted from single larvae in RIPA buffer containing protease inhibitors (Sigma). Whole-larval lysates were obtained by sonication in 100 μ l RIPA buffer using a Bioruptor Pico (Diagenode), 10 cycles of 10 sec on and 30 sec off. Proteins were quantified by bicinchoninic acid assay (BCA) assay; 30 μ g of protein of each sample were separated by SDS-PAGE (10%). Antibodies raised in rabbit against ALDH7A1 and c-Fos were obtained from Sigma (code A9860) and Santa Cruz biosciences (code sc-166940 X) and used at dilutions 1:2500 and 1:100, respectively, in 3% BSA. Anti-rabbit IgG, HRP-linked antibody was used in a dilution of 1:2000. The Clarity ECL Western

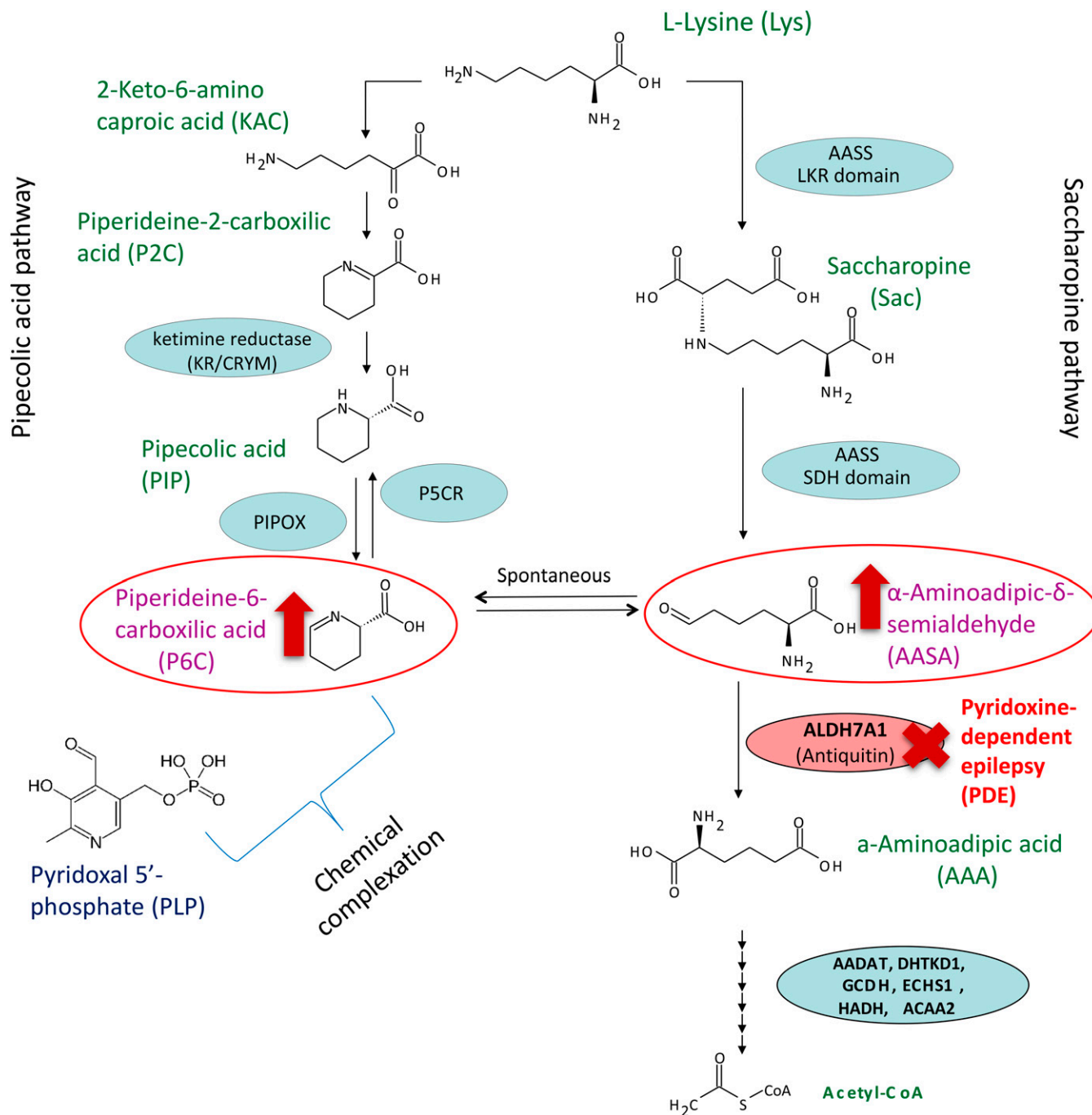


Figure 1 Pipecolic acid (left) and saccharopine (right) pathways for L-lysine catabolism in animals. The L-pipecolic acid pathway. LKR (lysine-ketoglutarate reductase) domain and SDH (saccharopine dehydrogenase) domain of the bifunctional AASS (aminoadipic semialdehyde synthase) enzyme. Antiquitin (encoded by the gene *ALDH7A1*) is deficient in pyridoxine-dependent epilepsy (red) leading to accumulation of AASA and P6C (red arrows). PIPOX (pipecolic acid oxidase). P5CR (piperideine-5-carboxylic reductase), encoded by the gene *PYCR1*. Further enzymatic steps convert AAA to Acetyl-CoA.

Blot Substrate kit (Bio-Rad, Hercules, CA) was used for chemiluminescent protein detection. Images were obtained and processed using the ChemiDoc Touch Imaging System (Bio-Rad).

Establishing mutant lines

CRISPR/Cas9 mutations were generated in WT zebrafish as described elsewhere (Hwang *et al.* 2013). The *aldh7a1*-targeting single-guide RNA (sgRNA) template plasmid was generated by

annealing oligonucleotides and ligation of the double-stranded DNA in the plasmid DR274 (Addgene, code 42250). The CRISPR target sequence (5'-GGACTTAAAGAGGACAATGA-3') and oligonucleotide design were performed using ZiFit software (Sander *et al.* 2010). To avoid off-target effects, we chose a target site with the lowest number of potential mutagenesis off-targets and with a minimum of three mismatches with such off-target sites. Plasmid sequences were checked by Sanger sequencing (ABI 3730).

The sgRNAs were transcribed from linearized template plasmids (Ambion MEGAscript T7/SP6) and purified (Promega, Madison, WI; Wizard SV Gel and PCR Clean-Up kit). The Cas9 protein was obtained from New England Biolabs (Beverly, MA). Fertilized one-cell-stage zebrafish eggs were injected with a mix containing ~300 ng/ μ l Cas9 protein and 15 ng/ μ l sgRNA. Embryos were raised and a portion of them (five pools of five embryos) were genotyped by heteroduplex melting assay (HMA) as described in Zhu *et al.* (2014). Briefly, primers flanking the CRISPR target site (forward sequence: “Gen1_FW,” 5'-ATGATGCAGCGCGTGCT GAC-3', reverse sequence: “Gen2_RV,” 5'-CCCTTTGAACCTC ACAGGAGTT-3') were used to amplify a segment of 434 bp. The PCR product was denatured and annealed. It was expected to contain a mixture of insertion/deletion mutations and WT alleles, which can form heteroduplex and homoduplex DNA. These can be easily identified by PAGE. The remaining embryos were raised to adulthood (F_0 generation) and backcrossed with WT fish. DNA was extracted from F_1 embryos to check for F_0 founders carrying specific mutations by HMA-PAGE. F_1 fish were raised to adulthood and heterozygous mutants were identified by fin clipping, followed by DNA extraction and HMA-PAGE. Potential mutants were sequenced allowing the identification of specific mutations (Figure S4). Populations of heterozygous F_1 fish carrying the same mutation were identified; the most common was a 5-nt insertion leading to a premature stop codon. F_1 heterozygous fish were backcrossed to WT fish to further eliminate potential off-target effects generated by the Cas9 nuclease. For the experiments described in this paper, we used crossings of F_2 heterozygous fish obtaining F_3 offspring containing a homozygous 5-nt deletion in the gene *aldh7a1*. The newly generated mutant allele was designated *aldh7a1^{ot100}* using the University of Ottawa designation and in accordance with the Zebrafish Information Network guidelines.

Larval fin clipping and multiplex PCR for genotyping

For genotyping of larvae to identify and distinguish the 5-nt insertion from the WT allele, we extracted genomic DNA from larval fins at 3–5 dpf and raised the corresponding larvae. Larval fin clipping was performed as an adaptation of a previously described protocol (Wilkinson *et al.* 2013). This method allowed genotyping and subsequent fin regeneration in a few days. Briefly, 3-dpf larvae were anesthetized in Tricaine, and then a microscalpel was used to section and obtain a microscopic caudal fin slice under a stereomicroscope (Nikon SMZ1500). The section was made by applying steady downward pressure to incise within the pigment gap site of the caudal fin, distal to the limit of the blood circulation. The fin was then placed in a small piece of filter paper, which was then submerged in 30 μ l of Chelex 5% solution in 96-well PCR plates. For tissue lysis, the samples were heated in a thermocycler at 95° for 15 min, then cooled to 4° for 10 min. The samples were centrifuged to pellet the Chelex beads leaving DNA in suspension. A 1.5 μ l volume of the DNA supernatant was used in each PCR reaction. This method allowed efficient recovery of DNA in 97% of the larvae on

average. A multiplex PCR reaction was used to precisely genotype WT and/or mutant alleles enabling the identification of fishes homozygous, heterozygous, or null for the 5-nt insertion mutation. This strategy is summarized in Figure S5, using the primers “Gen1_FW”: 5'-ATGATGCAGCGCGTGCT GAC-3', “Gen2_RV”: 5'-CCCTTTGAACCTCAGGAGTT-3', “5 nt-ins-specific_FW”: 5'-TGTTTTCAACGGTTCAACGG-3', and “WT-specific_RV”: 5'-TCCCTGTCCTCCCAAGAAC-3'. Three bands are expected using these four primers in a multiplex reaction: an ~430-bp amplicon resulted from amplification using Gen1_FW and Gen1_RV for both alleles, a 293-bp band specifically for the mutant allele, and a 195-bp band specifically for the WT allele (Figure S5). Samples were then run in an agarose 1% gel, stained with GelRed, and visualized under UV light, allowing discrimination of the different amplicons. We observed that the caudal fin regenerated in a few days (Figure S5, F and G) and normal development proceeded, as reported previously in Wilkinson *et al.* (2013).

RNA extraction and real-time PCR

Total RNA was extracted from three pools of five WT or *aldh7a1^{-/-}* larvae using the reagent QIAzol (QIAGEN, Valencia, CA) (each pool considered one biological replicate). First-strand-complementary DNA was synthesized from 1 μ g total RNA using the iScript kit (Bio-Rad). Quantitative real-time PCR was conducted using the following primer pairs: *gapdh* (5'-TGTTCCAGTACGACTCCACC-3' and 5'-ACCTGCATCACCCC ACTTAA-3'), *aldh7a1* (5'-TGTTCCAGATGGAGAGGC-3' and 5'-GGCTGTGATGATTCTACCAAG-C-3'), *gad1* (5'-AACTCAGGCGATTGTTGCAT-3' and 5'-CCAGCATCCTGAGG ACATTT-3'), and *gad2* (5'-AGCTGCTCTTGGA-ATCGGTA-3' and 5'-GCTGACAAAGAACGGCACGT-3'), with iQ SYBR Green Supermix (Bio-Rad). Relative mRNA levels were normalized to glyceraldehyde-3-phosphate dehydrogenase mRNA levels using the $\Delta\Delta$ CT method. The PCR amplification was performed in three technical replicates. The Student's *t*-test was used to evaluate the statistical significance of the differential mRNA levels between the three biological replicates of WT and *aldh7a1^{-/-}* siblings.

Morphological phenotyping

Larvae were photographed using a stereomicroscope (Nikon, Garden City; SMZ1500). Standard lengths (distance from the anterior tip of head to the base of the caudal fin) were measured manually using imageJ software.

Behavioral phenotyping

For locomotion tracking, 8 dpf and younger zebrafish larvae were placed in individual wells of a 96-well flat-bottomed culture dish (Corning); a 48-well flat-bottomed culture dish was used otherwise. For 96-well plates, each well contained 200 μ l of embryo medium, and 500 μ l for 48-well plates. Behavior was monitored at 28.5° using a ZebraBox system (ViewPoint Behavior Technology) consisting of a sound proof chamber with an infrared camera; analyses were performed

using Zebrolab locomotion tracking software (ViewPoint Behavior Technology). Larvae were allowed to acclimate to the plate and ZebraBox environment for 10 min. Five minutes of baseline were recorded followed by 5 min recording with light stimulus [five cycles of 10 sec on (100% light) and 50 sec off]. Using ZebraLab software, we calculated the distance traveled, duration, and number of high-speed [> 20 mm/sec (Afrikanova *et al.* 2013)], intermediate (8–20 mm/sec), and slow movements (< 8 mm/sec) for the 5-min baseline and 5 min light stimulus recordings. Larvae were plated each experiment in a randomized position to avoid bias. Videos were also analyzed blindly for the classification of seizure scores based on Baraban *et al.* (2005). GraphPad Prism was used to conduct ANOVA tests to compare the experimental groups.

Metabolite extraction and MS

For analysis of polar amino acids, each biological replicate consisted of pools of five deep-frozen 11-dpf larvae, which were sonicated in 150 μ l methanol and 75 μ l chloroform in 10 cycles (10 sec on, 30 sec off) using a Bioruptor Pico (Diagenode). Then, 112 μ l of chloroform and 112 μ l of H₂O were added to the lysate, vortexed, and centrifuged at 20000 \times g for 20 min at 4°, allowing phase separation. The supernatant containing polar metabolites was collected and dried under nitrogen. The metabolite extract was resuspended in HPLC-grade H₂O (Sigma) and used for liquid chromatography-MS analysis (LC-MSMS). P6C and pipercolic acid were measured using previously described methods (Struys *et al.* 2012a). AASA was measured using published methods (Mills *et al.* 2006). All analytes described in Figure S10 as part of the targeted amino acid panel were measured using LC-MSMS in the Newborn Screening Ontario-Inherited Metabolic Disease laboratory, using a method adapted from a published procedure (Waterval *et al.* 2009). For quantification of B6 vitamers, 300 μ l ice-cold trichloroacetic acid (TCA) solution (50 g/liter) was added to a pool of six deep-frozen zebrafish at 11 dpf. A small amount of zirconium oxide beads was added to the solution and put into a bullet blender for 5 min at level 8. Hereafter, the samples were centrifuged for 5 min at 13,000 rpm. The supernatant was prepared for the analysis of vitamin B6 vitamers using a published method (van der Ham *et al.* 2012), except that an 80- μ l volume of sample was used instead of 60 μ l [internal standard ratio (1:1)] and concentrations of the calibration solutions were 10 times lower than in the publication.

Electrophysiology

Electrophysiological recordings were obtained using methods described in the literature (Baraban *et al.* 2005). Specifically, 11-dpf zebrafish larvae were embedded in a 1.2% agarose gel prepared by dissolving low-melting temperature agarose in artificial CSF (aCSF) (NaCl 134 mM, KCl 2.9 mM, MgCl₂ 1.2 mM, CaCl₂ 2.1 mM, Glucose 10 mM, and HEPES 10 mM). Larvae were placed dorsal-up to give easy access to the brain. A waiting time of 15–20 min was allowed for the

zebrafish to become acclimated to the embedding. The bath volume was adjusted to 5 ml, and excess aCSF and gel were carefully removed to expose the top of the head. After transferring the larva to a chamber placed under a BX51WI Olympus microscope, a glass microelectrode was placed under visual guidance in the optic tectum of the fish. The glass microelectrode tip openings were ~ 2 μ m and were backfilled with 2 M NaCl. Electrical activity of the brain was amplified and low-pass filtered at 1 kHz with a MultiClamp 700B (Axon Instruments, Foster City, CA), digitized with a Digidata 1550 (Axon Instruments), and stored on a computer for later analysis. Traces were band-pass filtered (0.2–1 kHz). A detection threshold of three times background noise was applied to extract the events on a 5-min-long window. Detected events were manually sorted; those presenting two or more consecutive spikes were considered as seizure-like. Times and duration of each event were extracted. To test if movement artifacts were present, the neuromuscular blocker d-tubocurarine (15 μ M, Sigma) was used to paralyze larvae, added directly to the bathing medium (Figure S8).

Immunofluorescence

Fish larvae were sacrificed at 10 or 11 dpf and fixed in 4% PFA/PBS overnight at 4°. The samples were washed the following day with PBS three times, and equilibrated with a solution of 30% sucrose in PBS overnight at 4°. The samples were then incubated in a 1:2 30% sucrose: optimum cutting temperature (OCT) Compound (Tissue-Tek) solution for 30 min, frozen in cryomolds using liquid nitrogen, and then stocked at -20° for further sectioning. Transverse cryosections of 14–16 μ m of the whole head were obtained with a CM3050S cryostat (Leica, Concord, ON) and collected on microscope slides. All antibodies for the immunohistochemistry assay were previously validated. Sections were first rehydrated in PBS solution, and blocked in 10% calf serum in PBS-T (PBS plus 0.1% Tween 20) for 2 hr at room temperature. The primary rabbit anti-calretinin antibody (1:500, Swant7697) was incubated overnight at 4° in a 1% calf serum in PBS-T solution. Slides containing sections were then washed for 15 min 3 times with PBS-T, and incubated with the secondary antibody Alexa Fluor 488 goat anti-rabbit (1:1000, Invitrogen, Carlsbad, CA) protected from light for 2 hr at room temperature. Sections on slides were washed again three times with PBS-T and sealed and mounted with Vectashield mounting media (Vector Laboratories, Burlingame, CA) containing DAPI for nuclei staining. For each larval sample, every transverse section from the head was subjected to immunohistochemistry and visualized with a Zeiss ([Carl Zeiss], Thornwood, NY) AxioPhot fluorescence microscope, and images were acquired. Cells labeled with fluorescence were manually counted and the counts were crossed with an estimate number of cells using ImageJ.

Statistics

For multiple comparisons, one-way ANOVA with Tukey's test, or Kruskal–Wallis ANOVA with Dunn's *post hoc* test, were

used as appropriate. For pairwise comparisons, the Student's *t*-test was used. Significance testing and graphing was performed with GraphPad Prism 7 software. Processing of the chromatograms obtained by LC-MSMS was done using TargetLynx (Waters Associates, Milford, MA), including peak detection, peak integration, and concentration estimation based on calibration curves. For analysis of the MS amino acid panel, we used Metaboanalyst v3 (Xia *et al.* 2015), statistical analysis module for one-way ANOVA with Tukey's *post hoc* test, and the heatmap module to produce the heatmap representation (Figure S11) using Euclidean distance measure and Ward clustering algorithm.

Data availability

Sequences, plasmids, and the zebrafish line *aldh7a1*^{ot100} used in this study are available upon request. Figure legends and video descriptions for the supplemental material are contained in File S4. The authors state that all data necessary for confirming the conclusions presented in the article are represented fully within the article.

Results

Morpholino-based *aldh7a1* knockdown in zebrafish

The phenotypic impact of MO-based downregulation of *aldh7a1* in zebrafish was initially assessed; an MO molecule targeting the intron 4–exon 5 splice junction site (designated *aldh7a1*-SBMO-1) was designed to induce splice defects and therefore *aldh7a1* knockdown (Figure S2). First, 2.5 ng of either *aldh7a1*-SBMO-1 or control MO were injected in to one-cell-stage embryos and larvae collected at 4 dpf. Although the Aldh7a1 protein levels were knocked down to ~13% using the *aldh7a1*-SBMO-1 (Figure S3A), the morphant larvae displayed grossly normal morphology (Figure S3B) and did not differ in length, hatching time, or swimming behavior compared to controls. A second morpholino molecule (*aldh7a1*-MO1), used previously by Babcock *et al.* (2014), was also assessed. Although, as previously reported, a series of deformations were observed in the morphant larvae, western blot analysis failed to reveal any protein knockdown by this MO (Figure S3, F and G), indicating that these reported abnormalities are probably independent of *aldh7a1* function. In contrast, the successful knockdown of Aldh7a1 protein using the *aldh7a1*-SBMO-1 (Figure S3A) did not result in the phenotypes reported in Babcock *et al.* (2014), such as skeletal abnormalities and eye deformities (data not shown).

In an attempt to elicit a phenotype, *aldh7a1*-SBMO-1-injected larvae were exposed to lysine (20 mM) for 24 hr. We observed a significant increase in Aldh7a1 protein levels, partially overriding the inhibition caused by the morpholino (Figure S3C). However, the morphants did not accumulate the toxic PDE metabolite P6C in either control conditions or in the presence of lysine overload (Figure S3D). This suggests that low Aldh7a1 levels are sufficient for effective lysine metabolism, consistent with the known high catalytic efficiency

of this enzyme (Brocker *et al.* 2010; Kiyota *et al.* 2015). Therefore, we concluded that a complete loss-of-function of *aldh7a1* would be required to induce the AASA/P6C accumulation phenotype and thus PDE.

The *aldh7a1*^{ot100} allele leads to complete loss of functional Aldh7a1

By injecting single-cell zebrafish embryos with Cas9 protein and an *aldh7a1*-specific sgRNA, germline mutations were introduced in the first coding exon of the *Aldh7a1* gene. We identified and crossed F₀ founders with WT fish to generate F₁ zebrafish heterozygous for mutations in the *aldh7a1* gene. Identification of mutations was performed by a heteroduplex melting assay using PAGE gels. Sequencing of the CRISPR target region in the F₁ fish revealed the presence of several insertions or deletions in the *aldh7a1* gene (Figure S4).

We chose an F₁ heterozygous population carrying a 5-nt insertion mutation to generate F₂ fish by backcrossing with WT fish. Heterozygous F₂ fish were bred to generate homozygous mutants. The 5-nt insertion allele was easily detected by a multiplex PCR method allowing discrimination between WT, heterozygous, and *aldh7a1*^{-/-} (mutant) genotypes (Figure S5). F₃ offspring were sequenced to confirm the presence of homozygous mutants for the 5-nt insertion mutation in the *aldh7a1* gene (Figure 2, A and B). The insertion caused a frameshift in the primary *aldh7a1* transcript (GenBank: NM_212724), leading to a premature stop codon at position 50 of the translated protein sequence. This novel mutant was given the line designation *aldh7a1*^{ot100}. Fin clipping of randomly sorted F₃ larvae at 7 dpf was performed to extract DNA, and the whole larva was used to extract protein from the same animal. Western blotting showed successful Aldh7a1 protein knock-out in these fish (Figure 2C, lanes 1, 5, 6, and 9). As expected, heterozygous fish had approximately half of the normal Aldh7a1 protein levels compared to WT (Figure 2C). Multiplex PCR using the DNA samples extracted from the fins of the same fish confirmed each genotype (Figure 2D). The *aldh7a1* transcript in the mutants was 9% of that observed in the WT larvae, likely a result of nonsense-mediated mRNA decay (Figure S6).

Starting at 10 dpf, the mutants exhibited a hyperactive behavior characterized by fast swimming and convulsion-like activities, which intensified with time; these larvae all died by 14 dpf (Figure 2E). We tested two larval feeding protocols: one involving rotifer feeding from 6 dpf and one solely with the formulated zebrafish feed Gemma-75. Both elicited the same death phenotype (data not shown) and we chose to continue the experiments using the rotifer protocol. Although the morphology of the mutants from 0 to 10 dpf was indistinguishable from that of controls (WT and heterozygous), by the time of death, the mutants often displayed a ventrally-curved body phenotype (Figure 2F). As expected, the ablation of functional Aldh7a1 protein disrupted lysine degradation leading to the accumulation of AASA/P6C in the mutants. A representative LC-MSMS chromatogram of a control [WT or Het (Figure 2, G–H, top)] and a mutant larva

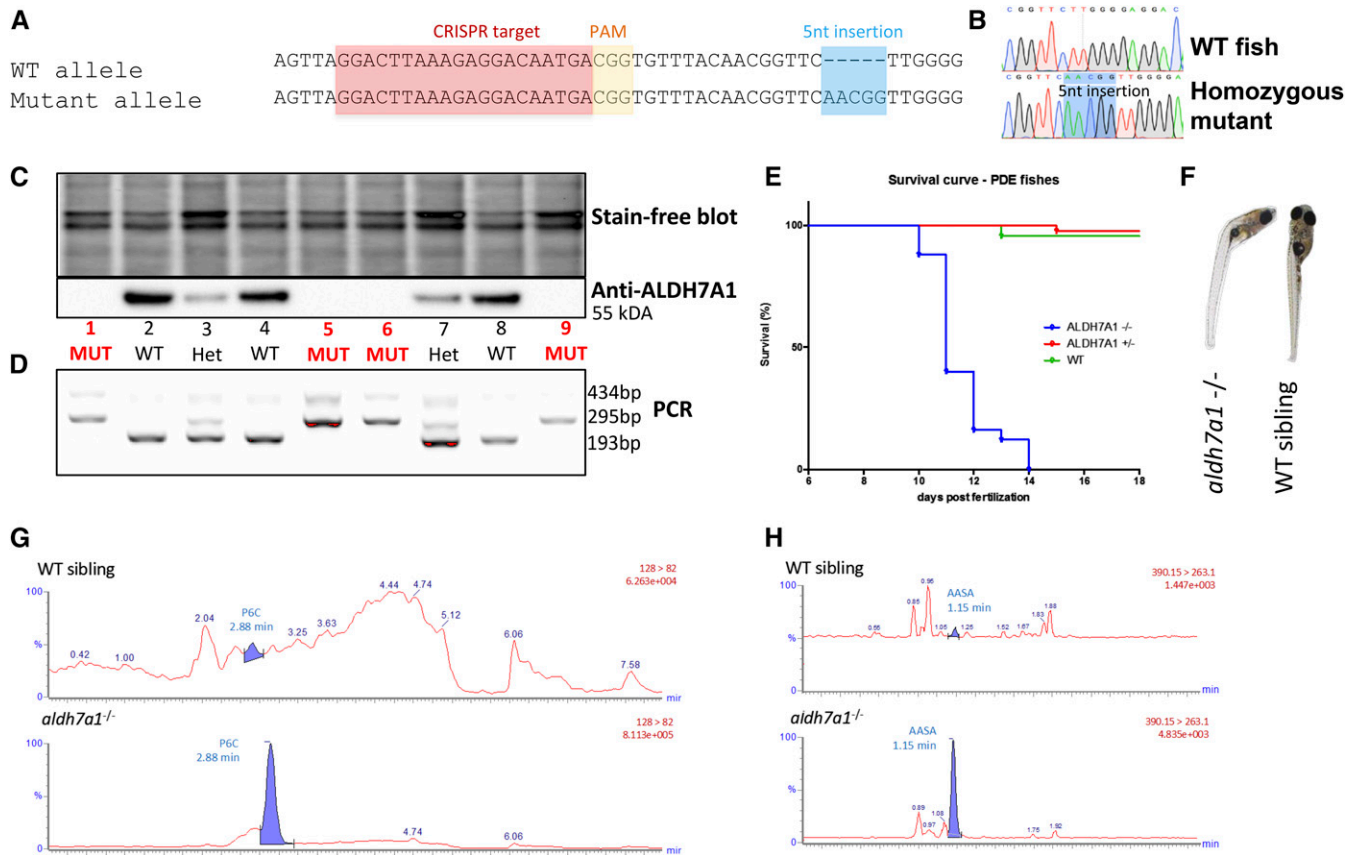


Figure 2 Development of an *aldh7a1*^{-/-} zebrafish model by CRISPR/Cas9. The allele *aldh7a1*^{ot100} contains a 5-nt insertion mutation (A), which leads to a premature stop codon and an N-terminal-truncated Aldh7a1 protein product. Sequencing chromatograms from F₃ larvae show the WT and homozygous mutant (B) patterns. Western blot detected the Aldh7a1 protein in WTs, with ~50% reduction and complete loss of expression in heterozygous and in the homozygous mutants, respectively (C). PCR-based genotyping (D) using DNA extracted from the fins of the larvae shown in (C) were consistent with the western findings. Kaplan–Meier survival plot showing early death in the homozygous mutants (11–14 dpf), $n = 12$ *aldh7a1*^{-/-}, $n = 18$ *aldh7a1*^{+/-}, $n = 10$ *aldh7a1*^{+/+} (E). Curved body phenotype observed at 11–14 dpf in the mutants after seizure onset (F). Representative liquid chromatography–mass spectrometry analysis of 7 dpf single larva ($n = 6$ per genotype); polar metabolite extracts revealed detection and accumulation of the PDE biomarkers P6C and AASA exclusively in the mutants (G and H bottom). No P6C or AASA signal was obtained in the extracts from WT or heterozygous siblings (G and H top). AASA, aminoadipate semialdehyde; CRISPR, clustered regularly interspaced short palindromic repeat; dpf, days postfertilization; HET, heterozygote; MUT, mutant; P6C, piperideine 6-carboxylate; PAM, protospacer adjacent motif; PDE, pyridoxine-dependent epilepsy; WT, wild-type.

(Figure 2, G–H, bottom) shows P6C and AASA detection in the micromolar range in the mutant larva. Heterozygous fish were indistinguishable from control WT fish and had normal lysine metabolism (data not shown), consistent with the hypothesis that this phenotype requires *aldh7a1* loss-of-function as seen in human patients with PDE.

Spontaneous seizure activity in *aldh7a1* mutant zebrafish

Epilepsy models in zebrafish larvae are characterized by seizure-like behavior ranging from episodes of excessive locomotor activity, sustained rhythmical jerking (clonus), and stiffening (tonus) to tonic–clonic seizures (Baraban *et al.* 2005, 2013; Hortopan *et al.* 2010; Teng *et al.* 2010). Normal movement behavior can be characterized as little (stage 0) or some swimming activity (stage 1), whereas seizure behavior is characterized as rapid “whirlpool-like” circling swimming (stage 2) and a series of whole-body convulsions culminating

in loss of posture (stage 3) (Baraban *et al.* 2005). Therefore, we monitored *aldh7a1* mutants for evidence of seizure-like behavior from video recordings. Larvae were genotyped by larval fin clipping at 3 dpf, fed on a rotifer diet from 6 dpf, and monitored using a high-speed infrared video tracking system (ZebraBox, ViewPoint Behavior Technology) in multi-well plates. Baseline and light stimulus recordings were performed daily from 7 to 14 dpf. There was no evidence of seizure-like behavior in fish of any genotype before 10 dpf. Video recordings starting in the evening of 10 dpf or in the morning of 11 dpf consistently showed signs of hyperactivity, with rapid “whirlpool-like” circular swimming (stage 2) and whole body-convulsions leading to loss of posture (stage 3) (Figure 3, A–D). We observed that hyperactivity/seizure-like behavior was immediately induced upon light stimulus in the *aldh7a1*^{-/-} fish, which spent more time (Figure 3A) and traveled greater distances (Figure 3B) in high-speed movements [traces shown in red in Figure 3C)] than WT and

heterozygous siblings. This was consistently observed in several batches of fish. No significant difference in quantified movement behavior was observed in 5-min baseline recordings analysis in either ambient light or darkness prior to the light stimulus, although spontaneous and sporadic convulsive behavior was consistently observed over > 10 batches of null-mutants. It is possible that the light induced convulsions in a more frequent and simultaneous fashion and thus facilitated the detection and quantification of the abnormal behavior. Examples of normal behavior in WT siblings and seizure-like behavior observed under microscope light in the mutant larvae are shown in [File S1](#) and [File S2](#), respectively. Blinded analysis of video recordings resulted in the identification of stages 2 and 3 of seizure behavior exclusively in the mutant fish (Figure 3D). Healthy larvae would only display stages 0 and 1, consistent with what is described in the literature (Baraban *et al.* 2005). The curved phenotype observed after seizure onset may be related to muscle stiffness, potentially derived from recurrent and uncontrolled tonic-clonic seizures.

We next tested whether the seizure-like behavior in *aldh7a1*^{-/-} mutants was associated with an electrographic component. Tectal field potential recordings from agar-immobilized 11-dpf larvae revealed spontaneous seizure-like events exclusively in *aldh7a1* mutants (*n* = 5) (Figure 3F). In contrast, WT or heterozygous siblings (*n* = 5) showed only normal electric activity (Figure 3E). In all mutants tested, we observed a high number of bursts of abnormal electrical discharge with long duration and high amplitude (Figure 3F), resembling the ictal-like activity described in other zebrafish and mammalian seizure models (Figure 3F, ii). In addition, short and low-amplitude bursts of interictal activity were also present (Figure 3F, iii). Representative recordings from additional *aldh7a1*^{-/-} mutants, negative control recordings from electrodes inserted into agar mounting medium, and movement artifacts not considered as spikes are illustrated in [Figure S7](#). We also obtained traces after paralyzing mutant larvae with d-tubocurarine, demonstrating the same features shown by the data in the absence of paralyzing agent, with no significant differences in the number and duration of events (*n* = 3 mutant larvae) ([Figure S8](#)). This further excludes the possibility of movement artifacts in our analysis. In summary, the seizure-like behavior, abnormal electrographic activity, and the early death phenotype are all consistent with an epilepsy phenotype in the *aldh7a1*^{-/-} larvae.

Pyr-dependent seizures in *aldh7a1*^{-/-} larvae

In humans, PDE manifests as intractable recurrent seizures that are significantly lessened by pharmacological doses of Pyr or PLP (Mills *et al.* 2006). We tested whether the *aldh7a1*^{-/-} larval epilepsy phenotypes described above responded to treatment with either compound. We observed a dose-dependent extension of the life span of the mutants with both PLP (Figure 4A) and Pyr (Figure 4B) at high doses. The median survival of 12 dpf for untreated mutants was increased up to 22 dpf with the PLP 500 μ M treatment. With daily treatment with millimolar doses of Pyr (5 and 10 mM), mutants sur-

vived until late juvenile stages (40 dpf), when the experiment was stopped. Therefore, high doses of either PLP or Pyr promote long-term survival of *aldh7a1*-null mutant fish. We chose to continue investigating Pyr (10 mM) responsiveness as it appeared to have a greater effect on life span, as well as being more stable, soluble, and less toxic than PLP. We observed that withdrawal of Pyr daily treatments would result in the appearance of the seizure behavior within 2–6 days and subsequent death (data not shown), highlighting the Pyr-dependency of the *aldh7a1*-null model.

We observed that the seizure-like behavior was prevented by Pyr treatment. Movement traces obtained from treated mutants under baseline (data not shown) and light stimulus conditions were indistinguishable from WT and Pyr-treated WT (Figure 4C). The duration and distance traveled in high-speed movements showed no statistical difference compared to WT and Pyr-treated WT, and all were significantly lower than in untreated mutants (Figure 4, D and E) (*P* = 0.0009 and 0.0019, ANOVA with Tukey's *post hoc* tests for pairwise comparisons). Blinded analysis of video recordings revealed that *aldh7a1*^{-/-} fish treated with Pyr did not display S2 and S3 stages of seizure behavior, hyperactivity, or high-speed movements, whether at baseline or under light stimulus (Figure 4, F and G). Additionally, the treated mutants did not display the curved body phenotype ([Figure S9](#)). Taken together, these results indicate the alleviation of the manifestations associated with the epilepsy phenotype with Pyr treatment. Video recordings showing the typical behavior of untreated and treated mutants can be seen in [File S2](#) and [File S3](#).

The electrophysiological burst characteristics were also compared between untreated (*n* = 5) and Pyr-treated mutants (*n* = 9; Figure 4, H–J). A statistically significant suppression of burst activity, measured as total event duration (*P* = 0.0207, Figure 4H) and number of events (*P* = 0.0348, Figure 4I) in a window of 5 min, was observed, suggesting Pyr-mediated amelioration of the spontaneous seizure phenotype (Kruskal–Wallis ANOVA with a Dunn's *post hoc* test). Given the time-consuming nature of this experiment and our ability to analyze only 4–5 larvae per day, four batches of larvae were analyzed, with consistent results. All untreated *aldh7a1*-null mutants displayed seizure-like bursts of electrical activity, whereas this was true for only 55% of the Pyr-treated mutants (5/9). Still, in the five Pyr-treated mutant fish displaying burst activity, it consisted of a lower number of events, as shown in Figure 4, H and I. Representative recordings of four Pyr-treated mutants are shown in Figure 4J. One Pyr-treated mutant displayed a high number of spikes (Figure 4J, third trace from top to bottom). These analyses were performed in ambient light and so we also tested whether light stimuli would further induce seizure-like activity in the untreated and treated mutants. Although the behavior of treated mutants was indistinguishable from WT siblings even after light stimuli, electrographic seizure events could be induced in the Pyr-treated mutants ([Figure S9](#)) and the burst activity was significantly higher than that recorded in ambient light.

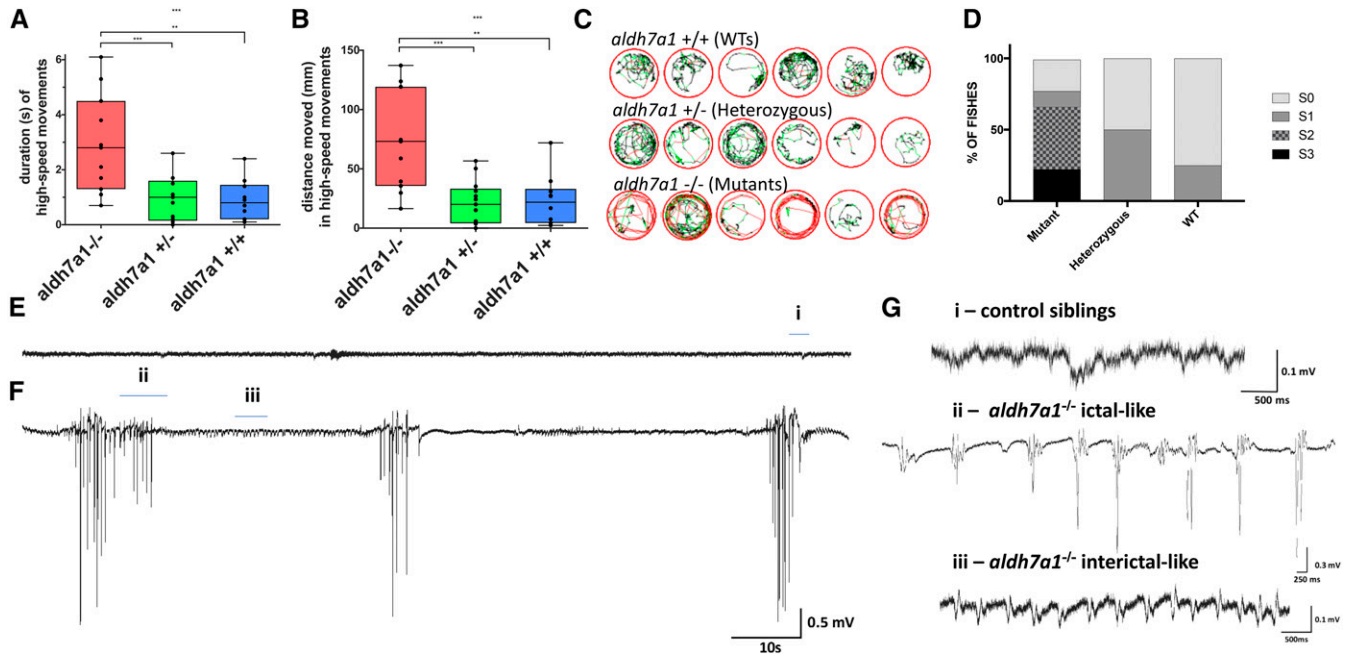


Figure 3 Seizure phenotype in *aldh7a1*^{-/-} 11-dpf larvae. Video recordings ($n = 12$ larvae per genotype) were analyzed for high-speed movement in the presence of light stimulus; the calculated duration (A) and distance traveled (B) are shown. Movement traces shown in red, green, and black represent high-speed, intermediate, and slow movements, respectively (C). Blinded classification of seizure scores from video recordings of mutants, heterozygous, and WT larvae ($n = 12$ larvae per genotype). S0 characterizes normal swimming behavior, S1 reflects increased activity, S2 indicates rapid circular swimming activity, and S3 represents whole-body convulsions. Tectal field recordings of representative 11-dpf WT sibling (E) and *aldh7a1*^{-/-} (F) showing spontaneous epileptiform-like electrographic activity in the mutants. Amplified view (G) of regions of the traces shown in (E and F): “i” normal activity as seen in WT and heterozygous siblings, “ii” ictal-like, and “iii” interictal-like epileptiform discharge observed in the mutants. Asterisks indicate statistical significance (* $P < 0.05$, ** $P < 0.01$, and *** $P < 0.001$) according to one-way ANOVA test on top of the graphics (in (A) $P = 0.0003$ and in (B) $P = 0.0002$) with Tukey’s *post hoc* pairwise tests. Error bars represent \pm SD. All experiments were performed comparing *aldh7a1*^{-/-} and its heterozygous or WT siblings. dpf, days postfertilization; WT, wild-type

In mammalian models, it is well established that almost all types of seizures cause dynamic alterations of immediate early genes, such as *c-fos*, in neurons located in seizure-initiation sites (Kiessling and Gass 1993). This has also been observed in zebrafish models of epilepsy (Baraban *et al.* 2005; Teng *et al.* 2011). We observed, by western blot analysis (Figure 4K), that *aldh7a1*^{-/-} larvae collected at 11 dpf displayed higher expression of *c-fos* compared to WT siblings and that this expression was normalized with Pyr treatment. Protein extracts from WT larvae treated with 15 mM of pentylentetrazole for 2 hr were used as positive controls for *c-fos* upregulation (Baraban *et al.* 2005) (Figure 4K, first two lanes). Therefore, we provide consistent evidence for Pyr responsiveness (survival, behavior, electrophysiology and *c-fos* expression) of the epileptic phenotype of *aldh7a1* mutants.

Lysine supplementation induces an earlier seizure phenotype

We next hypothesized that, since P6C accumulation leads to PLP inactivation and seizure occurrence, lysine supplementation would induce a more severe phenotype due to increased P6C production, quickly reaching a threshold necessary for PLP inactivation. The effects of lysine supplementation on mutant larvae before the onset (10 dpf) of the seizure-like behavior were assessed. We observed that mutants invariably

died within 48 hr of exposure to 20 mM lysine; Lys enrichment initiated at 6, 7, and 8 dpf in mutants lead to death of all larvae by 8, 9, and 10 dpf, respectively (Figure 5A). WT siblings, in contrast, were unaffected by lysine supplementation.

We then assessed whether the toxicity of AASA/P6C or the Pyr deficiency itself leads to persistent seizures and death. This was explored by assessing the impact of combining lysine overload with Pyr treatment. Mutants and WT siblings were supplemented at 8 dpf with lysine 20 mM and seizure-like behavior was monitored at 24 hr after the treatment (at 9 dpf). Two out of eight Lys-exposed mutants died after 24 hr of exposure, whereas the remaining six larvae clearly displayed seizure-like behavior (Figure 5) and died after 48 hr of exposure (Figure 5B). Pyr-untreated mutants died by 14 dpf as consistently observed previously. However, mutants treated with Pyr alone or in combination with Lys all survived until the end of this experiment (20 dpf), suggesting that it is the Pyr-deficiency, and not an unrelated AASA/P6C toxicity or other nonlysine-related *aldh7a1* loss-of-function, that underlies the seizure/death phenotype.

Early lysine-elicited seizure behavior was next quantified as outlined above. Lys-supplemented mutants (24 hr of exposure) displayed more high-speed movements at 9 dpf (Figure 5, C and D), whereas untreated, Pyr-treated, and Lys + Pyr-treated mutants of the same age did not display any evidence of

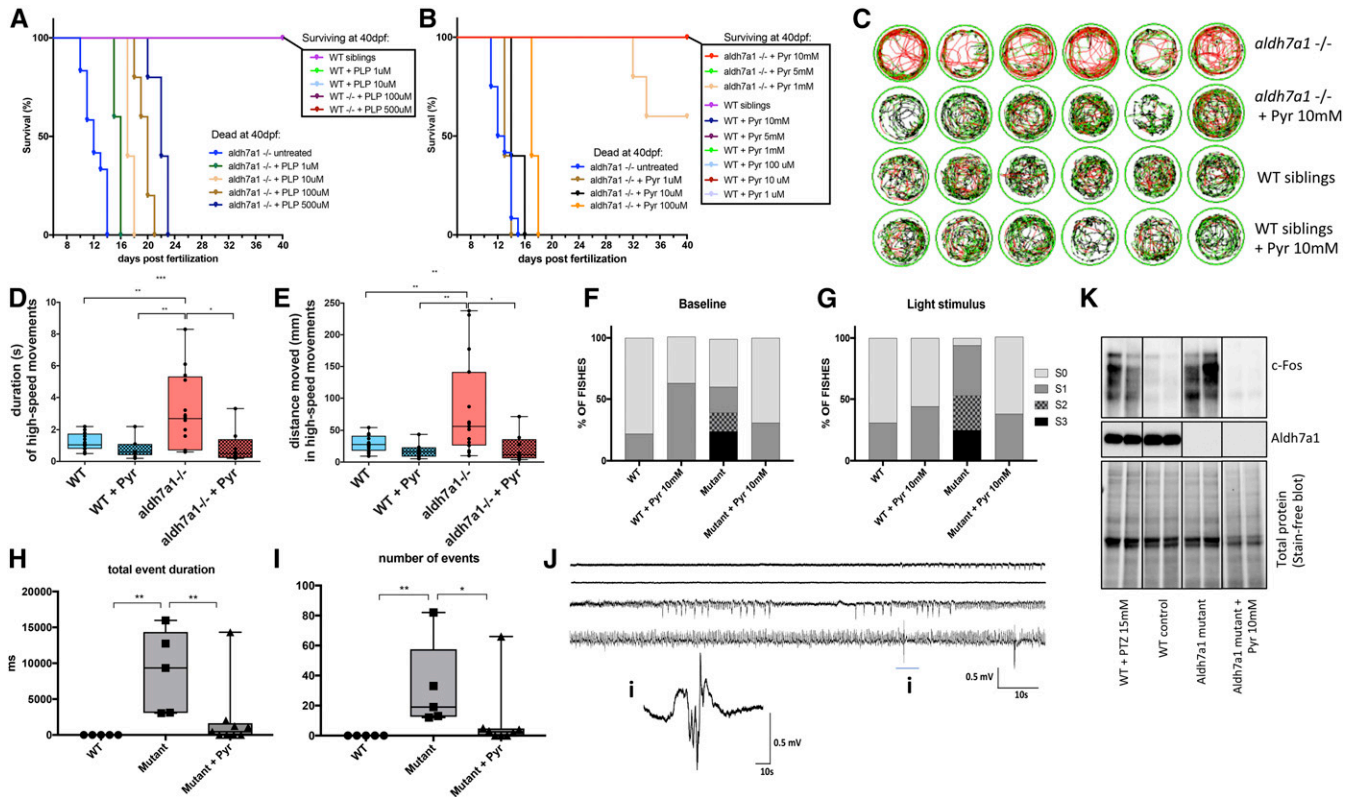


Figure 4 Pyridoxine (Pyr)-dependent epilepsy in *adh7a1*^{-/-} larvae. Pyridoxal 5'-phosphate (PLP) treatment promoted dose-dependent increase in survival of mutant larvae (A). Pyr treatment also led to prolonged life span of the null-mutants, with 100% survival until juvenile stage (5 and 10 mM daily) (B). In both cases, experiments were terminated at 40 days postfertilization (dpf) and consisted of *n* = 5 individuals per group except for untreated *adh7a1*^{-/-} (*n* = 12). Representative movement traces obtained from Zebralab software showing in red, high-speed, green, intermediate, and black, slow movements for mutants and their wild-type (WT) siblings, untreated and treated with Pyr 10 mM (C). Movement analysis using Zebralab showing duration (D) and distance traveled in high-speed movements (E). Blinded analysis of baseline (F) and light stimulus (G) video recordings classified the behavior in seizure scores as described previously. *N* = 16 *adh7a1*^{-/-} untreated, *n* = 8 *adh7a1*^{-/-} + Pyr 10 mM, *n* = 16 WT untreated, and *n* = 8 WT + Pyr 10 mM (D–G). Total event duration of the electrographic seizure-like bursts (H) and total number of such events (I) observed in a window of 5 min for *n* = 5 WT siblings, *n* = 5 untreated *adh7a1*^{-/-}, and *n* = 9 *adh7a1*^{-/-} treated with Pyr 10 mM. Examples of traces of treated mutants showing magnification of one burst are shown in “i” (J). Western blot probing with anti-c-Fos and anti-ALDH7A1 antibodies (K); each lane corresponds to protein extracts of a single larva. Asterisks indicate statistical significance (* *P* < 0.05, ** *P* < 0.01, and *** *P* < 0.001) based on ANOVA test with Tukey’s *post hoc* pairwise tests. Error bars represent ± SD. All experiments were performed comparing *adh7a1*^{-/-} and its WT siblings. Electrophysiology measurements were performed using four different batches of larvae.

seizure-like behavior. Time-course analysis suggested that the seizure onset occurred ~20 hr after addition of lysine (data not shown). This early seizure induction could also be seen in the movement diagrams obtained from Zebralab (Figure 5E) and was identified by blind video analysis, as all Lys-exposed mutants were classified as stages 2 or 3 (Figure 5F). These observations suggest the existence of a critical “seizure-inducing” AASA/P6C level, which is more rapidly attained with lysine supplementation.

Impairment of lysine metabolism in *adh7a1*^{-/-} larvae leading to low B6 vitamers and reduced GABA synthesis

LC-MSMS was next used to quantify lysine metabolites in polar extracts from mutant larvae and compare them with WT and heterozygous siblings. Several analytes could be detected and quantified in the extracts obtained from pools of five 11 dpf larvae using a targeted LC-MSMS amino acid panel (Figure S11). MetaboAnalyst 3.0 (Xia and Wishart 2002; Xia

et al. 2015) was used to study two different batches of *adh7a1*-null mutants (Mut1 and Mut2) compared with their respective batches of WT siblings (WT1 and WT2). Results of relative quantification (fold change) are shown in Figure S11 as a clustered heatmap visualization distinguishing WT and mutant samples based on patterns of cooccurrence of metabolites. One-way ANOVA and Tukey’s *post hoc* analysis of the four sample groups indicated 11 metabolites with statistical difference (Figure 6A). Four analytes showed consistently low levels in the two batches of *adh7a1*^{-/-} larvae compared to the two batches of WT larvae (Figure 6B): GABA, 2-aminobutyric acid, taurine, and methionine. The opposite pattern, high levels in mutants compared to WT, was found for seven compounds: P6C, saccharopine (SAC), pipercolate (PIP), tyrosine, β-alanine, serine, and citrulline.

Patients affected with PDE accumulate the toxic ALDH7A1 substrates AASA and P6C (Figure 1), which constitute both the main disease biomarkers and pathogenic drivers. Mutants

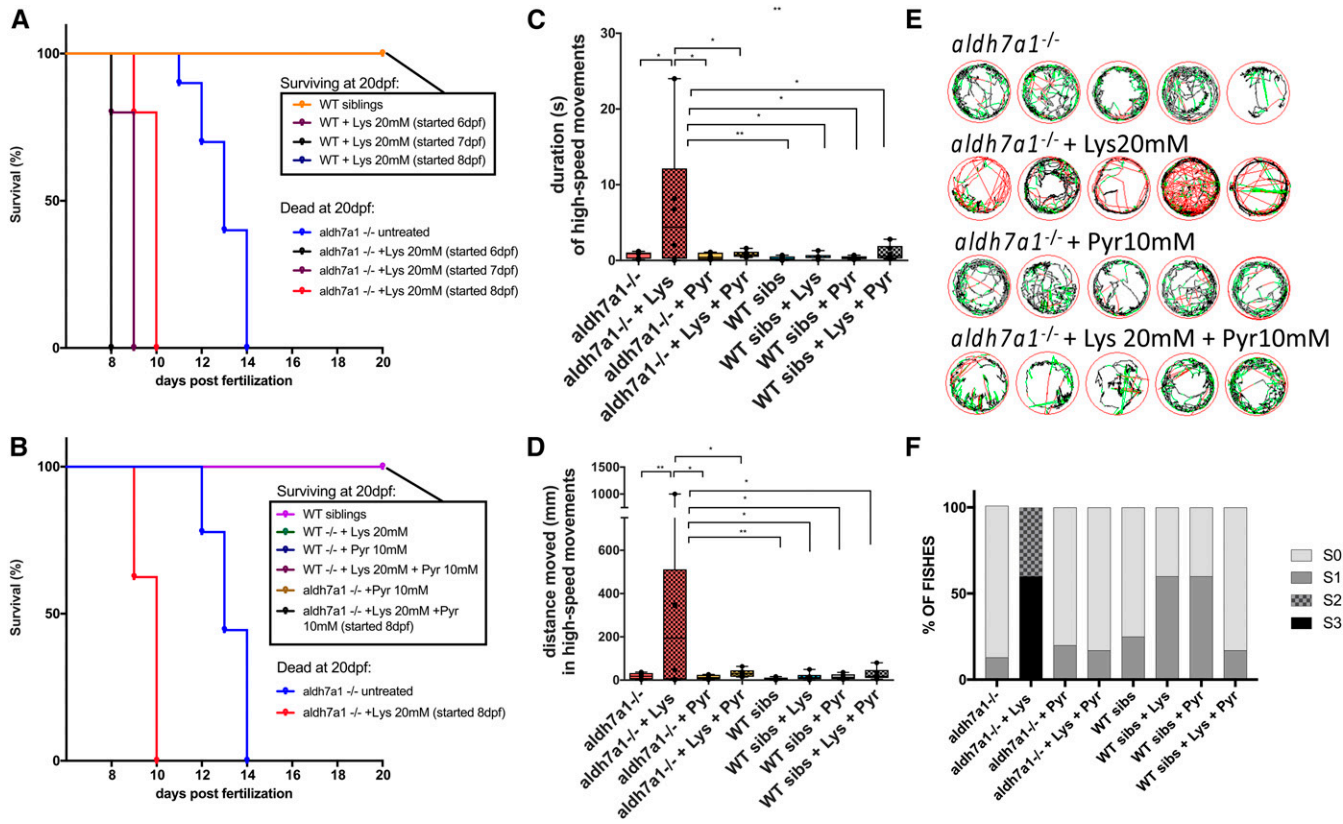


Figure 5 Early seizure onset and death following Lysine (Lys) treatment. Survival of *aldh7a1*^{-/-} and wild-type (WT) siblings after 48 hr of exposure with Lysine 20 mM (A) started at days 6, 7, or 8 days postfertilization (dpf). Survival of *aldh7a1*^{-/-} and WT siblings after 48 hr of treatment with Lys with or without daily Pyridoxine 10 mM (Pyr) treatments (B). Survival experiments were terminated at 20 dpf. Video analysis of 9-dpf larvae after 24 hr of treatment with Lys 20 mM, Pyr 10 mM, or both, showing significant increase in duration (C) and distance moved (D) in high-speed movements after light stimulus. Representative movement traces obtained from the Zebralab software at 9 dpf (24 hr after Lys treatment) showing the presence of larvae with hyperactivity and high-speed movements (red) (E). Blinded analysis of the same videos analyzed in (C–E) showing classification of each fish by seizure scores (S0, S1, S2, and S3), *n* = 8 larvae per group, except for mutant + Lys 20 mM where two fish died during the first 24 hr of treatment (F). Asterisks on top of the graph indicate statistical significance according to one-way ANOVA test [*P* = 0.0081 in (C) and *P* = 0.0060 in (D)] and asterisks comparing each pair of samples reflect Tukey's *post hoc* pairwise tests (* *P* < 0.05 and ** *P* < 0.01). Error bars represent ± SD.

accumulated AASA and P6C in the micromolar range in contrast to healthy heterozygous and WT larvae, in which this compound was undetectable (Figure 2 and Figure 6). Another lysine metabolite found elevated in a number of PDE patients is PIP (Plecko *et al.* 2005; Dalazen *et al.* 2014), possibly formed directly from the excess of P6C via the enzyme piperidine-5-carboxylic reductase (Figure 1) (Struys and Jakobs 2010; Neshich *et al.* 2013; Pena *et al.* 2017). PIP was also found to be elevated in mutant fish compared to controls (Figure 6B). To date, no publications have described the levels of SAC in PDE patients; SAC is the metabolite immediately upstream of AASA and P6C in the lysine degradation pathway. Here, we found 10-fold greater SAC levels (Figure 6B) in mutant larvae compared to controls. Elevated P6C levels could have reduced the catabolic flow via the SAC dehydrogenase domain of the amino adipic semialdehyde synthase enzyme (Figure 1). It is possible that SAC can be used as a potential novel biomarker for PDE diagnostics and/or monitoring of lysine degradation.

The amino acids shown in Figure 6B and that are not directly involved with the lysine degradation pathway are

potentially related to PLP-dependent enzymes for their synthesis or catabolism (Mills *et al.* 2011). Serine, for example, was found to be increased in the plasma of pyridoxamine 5'-phosphate oxidase (PNPO)-deficient patients [another disease leading to B6 deficiency (Mills *et al.* 2014)], and one hypothesis for its increase could be due reduced catabolism via serine dehydratase, a PLP-dependent enzyme (Mills *et al.* 2011). In addition, the diet provided to the zebrafish larvae might play an important role in the amino acid levels and patterns observed. Thus, rotifers (*B. plicatilis*) are rich in most amino acids (Srivastava *et al.* 2006) except for methionine, tryptophan, GABA, and citrulline. The amino acids obtained from their diet could have affected their metabolism through local or systemic B6 deficiency.

The conjugation of the accumulated P6C to PLP has been suggested to lead to the depletion of the latter, causing PLP deficiency (Mills *et al.* 2006). Therefore, we investigated if untreated mutants at 11 dpf would display lower systemic levels of PLP, as well as other vitamin B6 vitamers. We observed no significant changes in the levels of pyridoxine (Pyr),

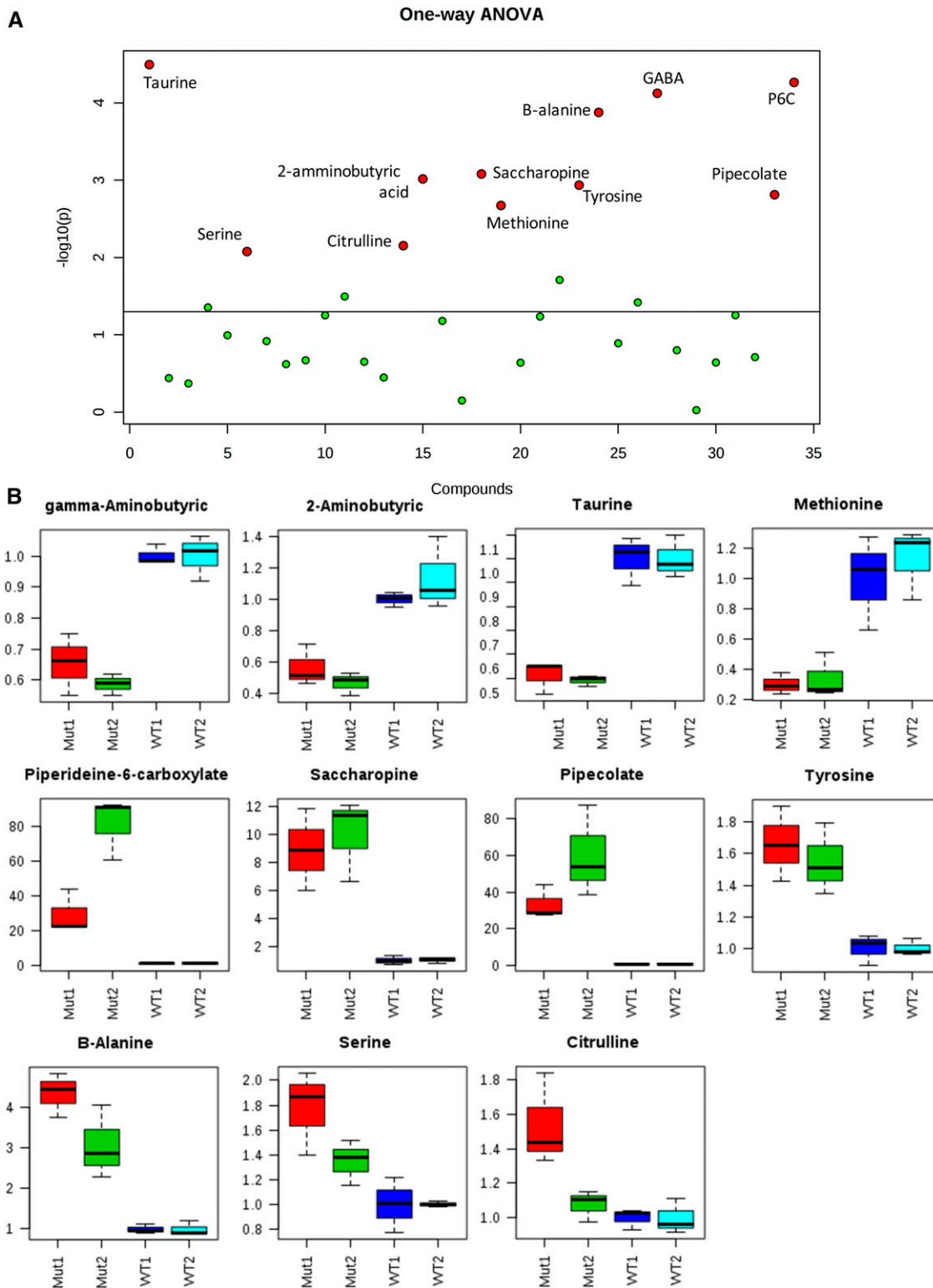


Figure 6 Targeted mass spectrometry allowed the identification of several amino acid perturbations when comparing two different batches of *aldh7a1*-null mutants (Mut1 and Mut2) and their WT siblings (WT1 and WT2). (A) Graphical summary of one-way ANOVA analysis comparing the four groups of samples, using P -value cutoff of 0.05. Metabolites identified with statistically significant changes are shown in red and labeled. (B) box and whisker plots summarize the normalized values (mean fold change \pm SD) for the metabolites shown in red in (B) significantly different between the two batches of WT and Mut. For this experiment, polar metabolite extracts of three pools (five 11-days postfertilization larvae each) were used for each group. GABA, γ -aminobutyric acid; P6C, piperideine 6-carboxylate; WT, wild-type.

pyridoxamine (PM), 4-pyridoxic acid, and Pyr 5'-phosphate (data not shown), but the null-mutants showed a statistically significant reduction in the levels of pyridoxal (PL, $P = 0.0094$, Figure 7A) and pyridoxamine 5'-phosphate (PMP, $P = 0.0013$, Figure 7B), and a reduction of PLP that almost reached statistical significance ($P = 0.0628$ Figure 7C) based on a Student's *t*-test. P6C is known to react with PLP and we expected to see mainly low PLP levels. Therefore, the large reductions of PMP and PL were unexpected. A possible condensation reaction between P6C or AASA and PMP or PLP has not been previously suggested. It is possible that reduced PL and PMP levels are due to a higher metabolic flux through the enzymes pyridoxal kinase and PNPO to replenish PLP. Since PL and PMP are direct precursors of PLP, transient PLP deficiency or local cerebral deficiency might possibly be occurring, despite its systemic levels appearing to be reduced by only ~30%.

Vitamin B6 deficiency is believed to be the main cause of seizures in PDE, as they are readily alleviated by Pyr treatment. One possible biological interpretation is based on the fact that PLP is the cofactor for glutamate decarboxylase (GAD), the enzyme responsible for synthesis of the central inhibitory neurotransmitter GABA (Figure 7D). Given that a sustained decrease in GABA levels can lead to seizures (Treiman 2001), it may be that a PLP-dependent reduction in the levels of active GAD (GAD^{PLP}) and thus in GABA levels, either locally in the brain or systemically, may underlie this key clinical feature of PDE (Figure 7D). In keeping with this, a previous study using skin fibroblasts isolated from PDE patients has suggested that these cells have impaired GABA synthesis compared to cells from healthy individuals (Gospe *et al.* 1994). We observed a reduction of ~50% of the levels of GABA in the 11-dpf *aldh7a1*-null mutants compared to controls in two different batches, as shown in Figure 6B. Therefore, assessed mutant larvae systemic GABA levels with or without Pyr treatment during the period that seizures are observed (*i.e.*, 11 dpf). As shown in Figure 8A, untreated *aldh7a1*^{-/-} larvae displayed a twofold reduction in systemic GABA levels relative to controls, and these levels were normalized under Pyr treatment.

We also observed that Pyr treatment did not significantly change the lysine degradation metabolite levels (PIP and SAC), but that P6C levels were reduced not normalized (Figure 8, B–D). Lysine levels were not significantly changed (ANOVA, data not shown). We also observed a strong correlation between P6C and lysine (Pearson's $r = 0.8442$, $P < 0.0001$), P6C and SAC ($r = 0.8941$, $P < 0.0001$), and P6C and PIP ($r = 0.874$, $P < 0.0001$) over measurements in two sets of mutant fish (data not shown). These results demonstrate a clear disruption of the lysine metabolic flow in the *aldh7a1*^{-/-} larvae, which is not rescued by Pyr treatment, reflecting what is seen in PDE patients.

We also investigated if there would be fewer GABAergic neurons in the larval brain at 11 dpf, given that such cells would likely be affected by persistent seizures, as previously reported in several models of other types of epilepsy (Tóth *et al.* 2010; Tóth and Maglóczy 2014). We did not observe a

significant difference in the number and organization of calretinin-positive cells in the telencephalon, diencephalon, mesencephalon, or rhombencephalon (Figure S12). Other GABA interneuron subpopulations might still be changed and this will be further investigated. It is possible that the strong regenerative capacity of the zebrafish brain may preclude the observation of slight decreases. Additionally, we did not observe a statistically significant difference between mRNA levels of *gad1b* and *gad2* by quantitative PCR when comparing WT and null-mutant larvae at 11 dpf (data not shown). These results may suggest that reduced PLP (or its precursors) leads to reduced GABA synthesis in the *aldh7a1*^{-/-} brain due to lowered GAD activity, rather than reduced GABA synthesis secondary to a loss of GABAergic neurons (here investigating the calretinin-positive population) or low GAD expression.

Discussion

PDE was initially described over 60 years ago (Hunt *et al.* 1954); we now present the first animal model of PDE, a zebrafish null for *aldh7a1*, manifesting dysregulated lysine metabolism with spontaneous seizure activity and premature death in the larval stage. The epileptic phenotype was responsive to Pyr and PLP treatments, which prolonged life span. The mutant fish accumulated the Aldh7a1 substrates AASA and P6C (Figure 1 and Figure 2) (the main PDE biomarkers); in contrast, morpholino-based knockdown of Aldh7a1 resulting in ~13% of normal protein levels did not result in either the accumulation of AASA/P6C (Figure S3) or any discernible larval phenotype. Thus, approximately one-tenth of normal Aldh7a1 activity may catalyze sufficient oxidation of AASA/P6C, preventing their accumulation to the toxic threshold that triggers PDE. In keeping with this observation, measurement of several heterologously-expressed missense-mutated Aldh7a1 proteins (pathogenic variants) in *Escherichia coli* were associated with < 3% of activity (Coulter-Mackie *et al.* 2012). For example, the E399Q mutation, which accounts for > 30% of the published human disease alleles (Plecko *et al.* 2007; Bennett *et al.* 2009; Mills *et al.* 2010), was reported to result in null Aldh7a1 enzymatic activity in overexpression assays using Chinese Hamster Ovary cells (Mills *et al.* 2006). These observations demonstrate the necessity of an *aldh7a1*-null model to study the pathogenesis of this rare condition in both the untreated and treated state.

Untreated *aldh7a1*^{-/-} mutant fish consistently displayed spontaneous seizures with convulsive behavior starting at 10 dpf and early death by 14 dpf. The reason why the seizure onset is consistently at 10 dpf remains unknown but some scenarios can be proposed. The maturation of the blood–brain barrier (BBB) has been demonstrated to occur in zebrafish from 3 to 10 dpf (Fleming *et al.* 2013). It is possible that the trapping of cerebrally-produced AASA and/or P6C (if impermeable to the BBB) after complete BBB maturation at 10 dpf could lead to seizure onset. A second possible scenario

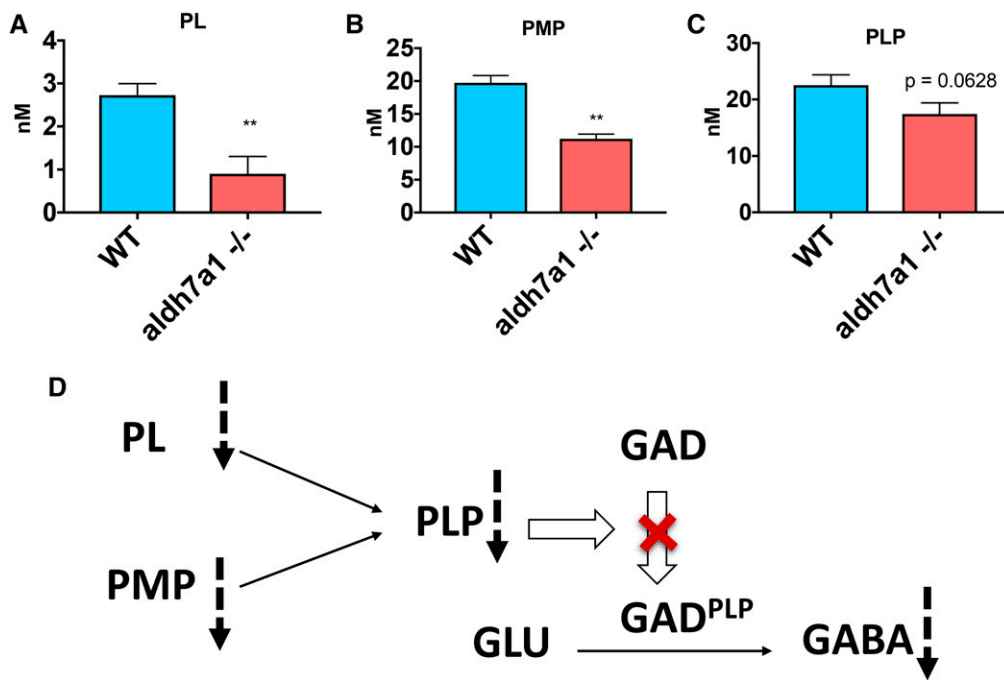


Figure 7 B6 vitamers are changed in *ald7a1*^{-/-} larvae compared to WT siblings. Lower levels of PL (A), PMP (B), and PLP (C) were observed in the null-mutants compared to WT according to liquid chromatography-mass spectrometry analysis using polar metabolite extracts (three replicates of six larvae pools). Asterisks indicate statistical significance according to Student's *t*-test (* *P* < 0.05 and ** *P* < 0.01). Error bars represent \pm SD. Possible mechanism for low GABA levels observed in the mutant larvae correlating with lower B6 vitamers levels (D), with potential reduction in the conversion levels of the inactive apo-form of GAD (and other PLP-dependent enzymes) to their catalytically active holo-form (GAD^{PLP}) by the covalent attachment of PLP. GABA, γ -aminobutyric acid; GAD, glutamate decarboxylase; PL, pyridoxal; PMP, pyridoxamine 5'-phosphate; PLP, pyridoxal 5'-phosphate; WT, wild-type.

could be that certain specific neuronal populations, more prone to seizures, might develop \sim 10 dpf. A third scenario could be that excess vitamin B6 that is maternally inherited and deposited in the yolk sac is depleted by PLP-P6C conjugation until 10 dpf. Finally, it may be that the seizure onset \sim 10 dpf simply occurs due to the fish obtaining lysine from their diet and thus reaching a threshold of AASA/P6C levels needed for PLP depletion [similar to what is hypothesized to occur in hyperprolinemia Type II (Farrant *et al.* 2001)]. Support for the threshold hypothesis comes from our observation that lysine supplementation accelerates seizure behavior and death (Figure 5). Pyr cotreatment was sufficient to rescue the larvae from seizures and mortality, in keeping with seizures that are indeed triggered by accelerated Pyr deficiency.

In our genetic model, tectal recordings revealed a complex electrographic seizure pattern resembling what is observed in mammalian models and in previously reported zebrafish epilepsy models (Baraban *et al.* 2013; Zhang *et al.* 2015; Grone *et al.* 2016; Sourbron *et al.* 2016). The observed electroencephalogram (EEG) profile in the *ald7a1*^{-/-} larvae consisted of frequent/brief interictal-like bursts and spontaneous ictal-like events with large-amplitude (minimum threefold higher than interictal-like) and long-duration spikes of electrical activity (hundreds of milliseconds), similar to seizure activity that is induced by the convulsing agent pentylenetetrazol (PTZ) (Baraban *et al.* 2005). Both electrographic spontaneous seizures and the convulsive-like behavior halted with Pyr (Figure 4), and the expression of c-Fos, an indicator of high neuronal activity and a gene highly expressed during seizures (Dragunow and Robertson 1987; Baraban *et al.* 2005; Teng *et al.* 2011), normalized. With-

drawal of Pyr treatment in fish larvae led to convulsive behavior and death within a week; seizure recurrence occurs between 1 and 51 days after withdrawal in PDE patients (Plecko *et al.* 2005; Mills *et al.* 2010; Yang *et al.* 2014). Interestingly, we observed the rapid intensification of larval convulsive behavior by light in untreated fish, and bursts of spikes without associated convulsive behavior could be induced even in treated fish (Figure S10). Photosensitive seizures have been observed in three molecularly-confirmed PDE patients based on clinical history, but photic stimulation via EEG studies has not yet been performed (personal communication, CDMvK). Families have also reported photosensitivity and/or light-triggered seizures in PDE patients (especially after exposure to flashes and intense light) despite Pyr treatment (personal communication with the Pyridoxine Dependent Epilepsy parent support group). In addition, several EEG abnormalities have been reported in PDE patients, which may remain despite B6 treatment (Mikati *et al.* 1991; Naasan *et al.* 2009; Bok *et al.* 2010; Schmitt *et al.* 2010; van Karnebeek and Jaggamantri 2015). More than three-quarters of individuals with PDE have or develop neurodevelopmental disabilities; whether this is a result of persistent subclinical EEG abnormalities, some other toxic effect of the elevated P6C, or some non-lysine-related function of ALDH7A1 remains to be determined. It may be that long-term behavioral and EEG phenotyping of our Pyr-treated mutant fish as they reach adulthood could shed light on this question.

In PDE, it is proposed that the accumulated levels of P6C undergo spontaneous Knoevenagel condensation with PLP, forming an inactive complex (P6C-PLP) that reduces the

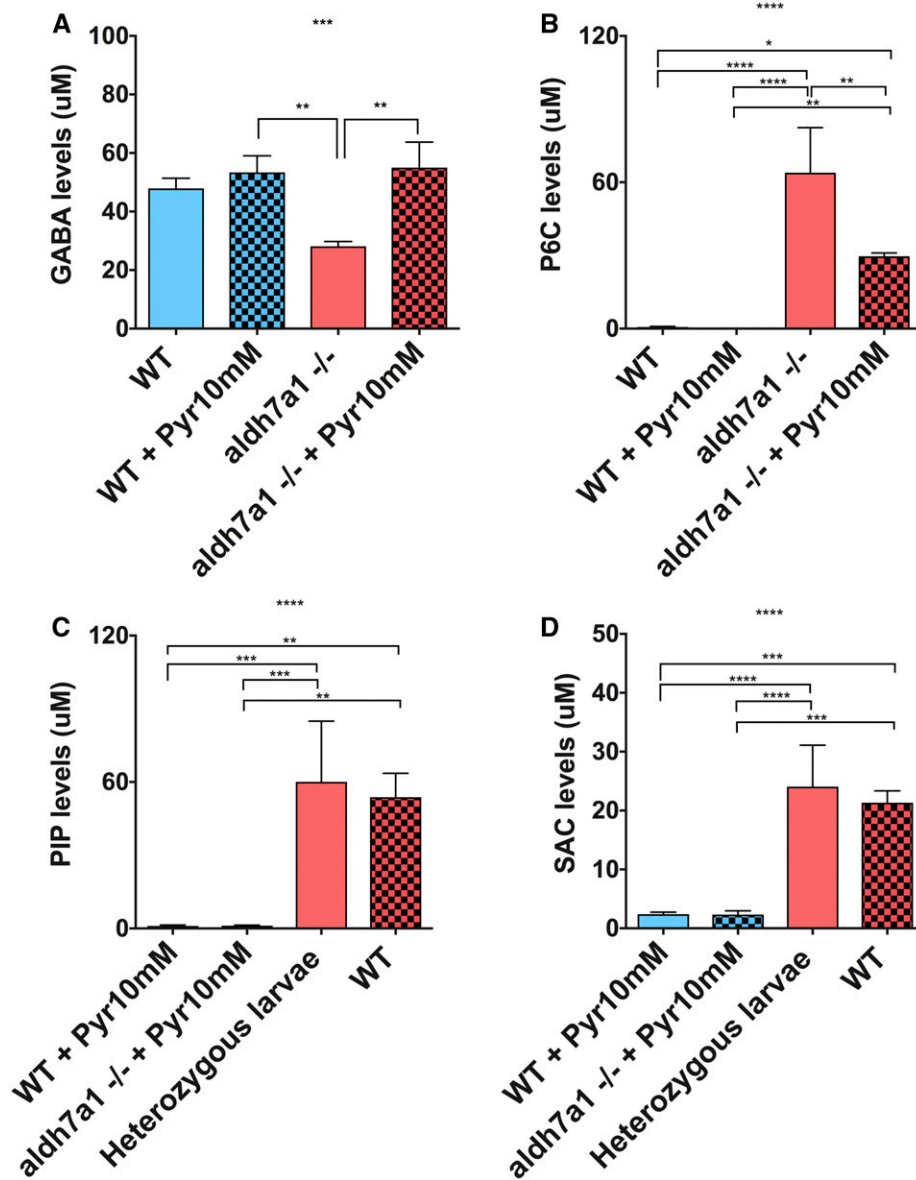


Figure 8 GABA levels are normalized by Pyr treatment but lysine metabolites are mostly unaffected in *aldh7a1*^{-/-} larvae. Mass spectrometry analysis of lysine metabolites in polar metabolite extracts was obtained from three pools of 11-days postfertilization larvae (six individuals each pool) per experimental condition; GABA (A), P6C (B), SAC (C), and PIP (D). Asterisks indicate statistical significance according to one-way ANOVA Tukey's *post hoc* tests (* $P < 0.05$, ** $P < 0.01$, *** $P < 0.001$, **** $P < 0.0001$). Error bars represent \pm SD. GABA, γ -aminobutyric acid; P6C, piperidine-6-carboxylate; PIP, pipercolic acid; Pyr, pyridoxine; SAC, saccharopine; WT, wild-type.

available PLP (Mills *et al.* 2006) in the CNS, and possibly systemically. PLP acts as a cofactor for over 140 enzymes, several of which are involved in amino acid and neurotransmitter metabolism (Percudani and Peracchi 2003; Clayton 2006); thus, it is not surprising that the neurodevelopmental and functional impact is significant. A similar impact is seen in children with Pyr-responsive epilepsy secondary to *PNPO* (MIM #610090) deficiency (Mills *et al.* 2005) or proline synthetase cotranscribed homolog (*PROSC*, MIM #617290) gene mutations (Darin *et al.* 2016). In both cases, it is believed that reduced PLP availability underlies the pathogenesis; specifically, due to reduced PLP synthesis in *PNPO* deficiency (Mills *et al.* 2005), and likely impaired cellular PLP homeostasis for *PROSC* deficiency (Darin *et al.* 2016). In hyperprolinemia type II (MIM #239510), a similar PLP (and likely other B6 vitamins) condensation with 1-pyrroline-5-carboxylate (structurally related to P6C) is observed, leading to low plasma PLP

levels and infantile seizures (Farrant *et al.* 2001). These disorders effectively capture the detrimental effects of functional PLP depletion. Correspondingly, we have observed a series of perturbations in amino acid levels, which might be related to low activity of PLP-dependent enzymes or deficient lysine metabolism (Figure 6).

It has been hypothesized that PLP deficiency leads to seizures secondary to its impact on a particularly important PLP-dependent enzyme, GAD, which is responsible for the biosynthesis of GABA, the main cerebral inhibitory neurotransmitter. Indeed, low GABA production due to PLP deficiency was proposed as the underlying mechanism for Pyr-dependent seizures long before the discovery of the genetic causes of PDE (Kurlemann *et al.* 1992; Gospe *et al.* 1994; Goto *et al.* 2001). However, measurement of GABA and PLP levels in PDE patients have yielded inconsistent results: low CSF/cerebral levels found in two studies (Lott *et al.* 1978;

Mills *et al.* 2011) and normal CSF, plasma, and urine levels reported by others (Goto *et al.* 2001; Footitt *et al.* 2013). One possible limitation in the investigation of PLP and GABA levels in patients is that the ongoing B6 treatment and B6 administration regimen may mask persistent depletions. In addition, PLP and GABA depletion in PDE may be localized to specific brain compartments and intracellular changes may not necessarily be captured using CSF measurements. By studying untreated *aldh7a1*^{-/-} fish, we observed a reduction of B6 vitamers (PLP, PMP, and PL) (Figure 7), and an approximate halving of systemic GABA levels relative to WT siblings (Figure 6 and Figure 8). Furthermore, the unanticipated observation of low PMP and PL levels (~1.8-fold and threefold reduction, respectively) might indicate the novel possibility of AASA and/or P6C reacting with these B6 vitamers leading to their inactivation. Another possibility might be that PL and PMP are being rapidly metabolized by the enzymes pyridoxal kinase and PNPO in the body's homeostatic attempt to replenish PLP and thus have reduced levels. Not surprisingly, several other amino acids also showed significant change, and it is possible that many other metabolic pathways are disturbed in *Aldh7a1* deficiency. Ultimately, GABA levels in the mutants normalized remarkably under Pyr treatment (Figure 8) and the seizure phenotype was halted (Figure 4).

There are no other reports of animal models for *aldh7a1*-deficiency or PDE in the literature, but other genetic or pharmacological models displaying Pyr-responsive seizures (PRS) have been described. For example, Ginkotoxin acts as an inhibitor of PLP synthesis and ginkotoxin-phosphate as a competitive inhibitor for PLP (Lee *et al.* 2012). Zebrafish larvae (5–7 dpf) treated with ginkotoxin develop seizure-like behavior that is reversed by PLP and/or GABA treatment, further supporting a role of PLP and GABA deficiency in seizure pathogenesis (Lee *et al.* 2012). The PLP ecto-phosphatase activity of the enzyme TNSALP (tissue-nonspecific alkaline phosphatase, OMIM #171760) is likely related to the PRS observed in *TNSALP* deficiency (Weiss *et al.* 1988). Mice deficient for *TNSALP* display seizures and early death by 2 weeks of age, with low PLP and GABA levels (50% reduction) detected in the brain as the potential epilepsy-triggering mechanism (Waymire *et al.* 1995). Imbalance in GABA levels could be possibly related to the seizure phenotype in these diseases, in PDE, and in our zebrafish model. It is also possible that other metabolites altered as a consequence of *Aldh7a1* deficiency and/or PLP deficiency can also play a role in seizures, and this will be studied in the future. Additional studies investigating levels of other neurotransmitters and other AASA/P6C toxicity effects could also provide alternative and/or complementary explanations for the mechanisms underlying seizure occurrence.

In conclusion, the *aldh7a1*^{-/-} fish constitute a faithful model for PDE and thus represent an important tool for an improved understanding of PDE pathogenesis. Given the Pyr dependency of the animals, there will be opportunities to study the pathogenesis and biochemistry of this disease, not only in larvae but in juvenile and adult stages as well. One unique advantage is the “drug inducibility” of our model,

i.e., the ability to withdraw Pyr treatment at any given time and study the dynamics of PDE pathogenesis. Although our analysis strongly suggests that the primary driver of PDE pathogenesis arises from AASA/P6C accumulation due to *Aldh7a1* ablation, impairment in other functions of this enzyme [*e.g.*, involvement in oxidative stress (Brocker *et al.* 2011), osmotic stress (Brocker *et al.* 2010), and cell growth/DNA protection (Chan *et al.* 2011)] may also play a role. Our results also give further support to the theory that lysine, in excess, is toxic for PDE patients. Finally, our model can now be used for drug screening and testing of new therapies, to potentially identify drugs that can add to the pyridoxine treatment to further control seizure activity and improve the neurodevelopmental outcomes for these children.

Acknowledgments

The authors would like to thank the patients and families living with pyridoxine-dependent epilepsy who give this work meaning. They also thank William Fletcher and Christine Archer for the support with zebrafish care and helpful discussions, Sandra Noble for sharing CRISPR/Cas9 protocols and reagents, and Sarah Schock for critically reviewing this manuscript. The authors thank the Rare Disease Models and Mechanism Network [funded by the Canadian Institutes of Health Research (CIHR) and Genome Canada] and the Care4Rare Canada Consortium (funded by Genome Canada, CIHR, Ontario Genomics, Ontario Research Fund, and the Children's Hospital of Eastern Ontario Foundation) for financially supporting this research. I.A.P. is supported by a CIHR postdoctoral fellowship award.

Literature Cited

- Afrikanova, T., A.-S. K. Serruys, O. E. M. Buenafe, R. Clinckers, I. Smolders *et al.*, 2013 Validation of the zebrafish pentylenetetrazol seizure model: locomotor versus electrographic responses to antiepileptic drugs. *PLoS One* 8: e54166.
- Babcock, H. E., S. Dutta, R. P. Alur, C. Brocker, V. Vasiliou *et al.*, 2014 *aldh7a1* regulates eye and limb development in zebrafish. *PLoS One* 9: e101782.
- Baraban, S. C., M. R. Taylor, P. A. Castro, and H. Baier, 2005 Pentylenetetrazole induced changes in zebrafish behavior, neural activity and c-fos expression. *Neuroscience* 131: 759–768.
- Baraban, S. C., M. T. Dinday, and G. A. Hortopan, 2013 Drug screening in *Scn1a* zebrafish mutant identifies clemizole as a potential Dravet syndrome treatment. *Nat. Commun.* 4: 2410.
- Baxter, P., 2001 Pyridoxine-dependent and pyridoxine-responsive seizures. *Dev. Med. Child Neurol.* 43: 416–420.
- Bennett, C. L., Y. Chen, S. Hahn, I. A. Glass, and S. M. J. Gospe, 2009 Prevalence of *ALDH7A1* mutations in 18 North American pyridoxine-dependent seizure (PDS) patients. *Epilepsia* 50: 1167–1175.
- Bok, L. A., N. M. Maurits, M. A. Willemsen, C. Jakobs, L. K. Teune *et al.*, 2010 The EEG response to pyridoxine-IV neither identifies nor excludes pyridoxine-dependent epilepsy. *Epilepsia* 51: 2406–2411.

- Brocker, C., N. Lassen, T. Estey, A. Pappa, M. Cantore *et al.*, 2010 Aldehyde dehydrogenase 7A1 (ALDH7A1) is a novel enzyme involved in cellular defense against hyperosmotic stress. *J. Biol. Chem.* 285: 18452–18463.
- Brocker, C., M. Cantore, P. Failli, and V. Vasilou, 2011 Aldehyde dehydrogenase 7A1 (ALDH7A1) attenuates reactive aldehyde and oxidative stress induced cytotoxicity. *Chem. Biol. Interact.* 191: 269–277.
- Chan, C.-L., J. W. Y. Wong, C.-P. Wong, M. K. L. Chan, and W.-P. Fong, 2011 Human antiquitin: structural and functional studies. *Chem. Biol. Interact.* 191: 165–170.
- Clayton, P. T., 2006 B6-responsive disorders: a model of vitamin dependency. *J. Inherit. Metab. Dis.* 29: 317–326.
- Coughlin, II, C. R., C. D. M. van Karnebeek, W. Al-Hertani, A. Y. Shuen, S. Jaggamantri *et al.*, 2015 Triple therapy with pyridoxine, arginine supplementation and dietary lysine restriction in pyridoxine-dependent epilepsy: neurodevelopmental outcome. *Mol. Genet. Metab.* 116: 35–43.
- Coulter-Mackie, M. B., A. Li, Q. Lian, E. Struys, S. Stockler *et al.*, 2012 Overexpression of human antiquitin in *E. coli*: enzymatic characterization of twelve ALDH7A1 missense mutations associated with pyridoxine-dependent epilepsy. *Mol. Genet. Metab.* 106: 478–481.
- Dalazen, G. R., M. Terra, C. E. D. Jacques, J. G. Coelho, R. Freitas *et al.*, 2014 Pipecolic acid induces oxidative stress in vitro in cerebral cortex of young rats and the protective role of lipoic acid. *Metab. Brain Dis.* 29: 175–183.
- Darin, N., E. Reid, L. Prunetti, L. Samuelsson, R. A. Husain *et al.*, 2016 Mutations in PROSC disrupt cellular pyridoxal phosphate homeostasis and cause vitamin-B6-dependent epilepsy. *Am. J. Hum. Genet.* 99: 1325–1337.
- Dragunow, M., and H. A. Robertson, 1987 Kindling stimulation induces c-fos protein(s) in granule cells of the rat dentate gyrus. *Nature* 329: 441–442.
- Farrant, R. D., V. Walker, G. A. Mills, J. M. Mellor, and G. J. Langley, 2001 Pyridoxal phosphate de-activation by pyrroline-5-carboxylic acid. Increased risk of vitamin B6 deficiency and seizures in hyperprolinemia type II. *J. Biol. Chem.* 276: 15107–15116.
- Fleming, A., H. Diekmann, and P. Goldsmith, 2013 Functional characterisation of the maturation of the blood-brain barrier in larval zebrafish. *PLoS One* 8: e77548.
- Footitt, E. J., P. T. Clayton, K. Mills, S. J. Heales, V. Neergheen *et al.*, 2013 Measurement of plasma B6 vitamers profiles in children with inborn errors of vitamin B6 metabolism using an LC-MS/MS method. *J. Inherit. Metab. Dis.* 36: 139–145.
- Gospe, S. M., 2017 Pyridoxine-dependent epilepsy. *GeneReviews*® [Internet]. Available at: <https://www.ncbi.nlm.nih.gov/books/NBK1486/>. Accessed July, 2017.
- Gospe, S. M. J., K. L. Olin, and C. L. Keen, 1994 Reduced GABA synthesis in pyridoxine-dependent seizures. *Lancet (London, England)* 343: 1133–1134.
- Goto, T., N. Matsuo, and T. Takahashi, 2001 CSF glutamate/GABA concentrations in pyridoxine-dependent seizures: etiology of pyridoxine-dependent seizures and the mechanisms of pyridoxine action in seizure control. *Brain Dev.* 23: 24–29.
- Griffin, A., K. R. Hamling, K. Knupp, S. Hong, L. P. Lee *et al.*, 2017 Clemizole and modulators of serotonin signalling suppress seizures in Dravet syndrome. *Brain* 140: 669–683.
- Grone, B. P., M. Marchese, K. R. Hamling, M. G. Kumar, C. S. Krasniak *et al.*, 2016 Epilepsy, behavioral abnormalities, and physiological comorbidities in syntaxin-binding protein 1 (STXBPI) mutant zebrafish. *PLoS One* 11: e0151148.
- Hortopan, G. A., M. T. Dinday, and S. C. Baraban, 2010 Spontaneous seizures and altered gene expression in GABA signaling pathways in a mind bomb mutant zebrafish. *J. Neurosci.* 30: 13718–13728.
- Hunt, A. D. J., J. J. Stokes, W. W. McCrory, and H. H. Stroud, 1954 Pyridoxine dependency: report of a case of intractable convulsions in an infant controlled by pyridoxine. *Pediatrics* 13: 140–145.
- Hwang, W. Y., Y. Fu, D. Reyon, M. L. Maeder, S. Q. Tsai *et al.*, 2013 Efficient genome editing in zebrafish using a CRISPR-Cas system. *Nat. Biotechnol.* 31: 227–229.
- Kiessling, M., and P. Gass, 1993 Immediate early gene expression in experimental epilepsy. *Brain Pathol.* 3: 381–393.
- Kiyota, E., I. A. Pena, and P. Arruda, 2015 The saccharopine pathway in seed development and stress response of maize. *Plant Cell Environ.* 38: 2450–2461.
- Kurlemann, G., R. Ziegler, M. Gruneberg, T. Bommelburg, K. Ullrich *et al.*, 1992 Disturbance of GABA metabolism in pyridoxine-dependent seizures. *Neuropediatrics* 23: 257–259.
- Lee, G.-H., S.-Y. Sung, W.-N. Chang, T.-T. Kao, H.-C. Du *et al.*, 2012 Zebrafish larvae exposed to ginkgotoxin exhibit seizure-like behavior that is relieved by pyridoxal-5'-phosphate, GABA and anti-epileptic drugs. *Dis. Model. Mech.* 5: 785–795.
- Lee, P., W. Kuhl, T. Gelbart, T. Kamimura, C. West *et al.*, 1994 Homology between a human protein and a protein of the green garden pea. *Genomics* 21: 371–378.
- Lott, I. T., T. Coulombe, R. V. Di Paolo, E. P. J. Richardson, and H. L. Levy, 1978 Vitamin B6-dependent seizures: pathology and chemical findings in brain. *Neurology* 28: 47–54.
- Mercimek-Mahmutoglu, S., D. Cordeiro, V. Cruz, K. Hyland, E. A. Struys *et al.*, 2014 Novel therapy for pyridoxine dependent epilepsy due to ALDH7A1 genetic defect: L-arginine supplementation alternative to lysine-restricted diet. *Eur. J. Paediatr. Neurol.* 18: 741–746.
- Mikati, M. A., E. Trevathan, K. S. Krishnamoorthy, and C. T. Lombroso, 1991 Pyridoxine-dependent epilepsy: EEG investigations and long-term follow-up. *Electroencephalogr. Clin. Neurophysiol.* 78: 215–221.
- Mills, P., E. Footitt, and P. T. Clayton, 2011 Vitamin B6 metabolism and inborn errors. *The Online Metabolic and Molecular Bases of Inherited Disease*. Available at: <http://ommbid.mhmedical.com/content.aspx?bookid=971§ionid=62646411>. Accessed July, 2017.
- Mills, P. B., R. A. H. Surtees, M. P. Champion, C. E. Beesley, N. Dalton *et al.*, 2005 Neonatal epileptic encephalopathy caused by mutations in the PNPO gene encoding pyridox(am)ine 5'-phosphate oxidase. *Hum. Mol. Genet.* 14: 1077–1086.
- Mills, P. B., E. Struys, C. Jakobs, B. Plecko, P. Baxter *et al.*, 2006 Mutations in antiquitin in individuals with pyridoxine-dependent seizures. *Nat. Med.* 12: 307–309.
- Mills, P. B., E. J. Footitt, K. A. Mills, K. Tuschl, S. Aylett *et al.*, 2010 Genotypic and phenotypic spectrum of pyridoxine-dependent epilepsy (ALDH7A1 deficiency). *Brain* 133: 2148–2159.
- Mills, P. B., S. S. M. Camuzeaux, E. J. Footitt, K. A. Mills, P. Gissen *et al.*, 2014 Epilepsy due to PNPO mutations: genotype, environment and treatment affect presentation and outcome. *Brain* 137: 1350–1360.
- Naasan, G., M. Yabroudi, A. Rahi, and M. A. Mikati, 2009 Electroencephalographic changes in pyridoxine-dependent epilepsy: new observations. *Epileptic Disord.* 11: 293–300.
- Neshich, I. A. P., E. Kiyota, and P. Arruda, 2013 Genome-wide analysis of lysine catabolism in bacteria reveals new connections with osmotic stress resistance. *ISME J.* 7: 2400–2410.
- Pena, I. A., A. MacKenzie, and C. D. M. Van Karnebeek, 2016 Current knowledge for pyridoxine-dependent epilepsy: a 2016 update. *Expert Rev. Endocrinol. Metab.* 12: 1–16.
- Pena, I. A., L. A. Marques, A. B. A. Laranjeira, J. A. Yunes, M. N. Eberlin *et al.*, 2017 Mouse lysine catabolism to amino adipate occurs primarily through the saccharopine pathway; implications for pyridoxine dependent epilepsy (PDE). *Biochim. Biophys. Acta* 1863: 121–128.
- Percudani, R., and A. Peracchi, 2003 A genomic overview of pyridoxal-phosphate-dependent enzymes. *EMBO Rep.* 4: 850–854.

- Plecko, B., C. Hikel, G. Korenke, B. Schmitt, M. Baumgartner *et al.*, 2005 Pipecolic acid as a diagnostic marker of pyridoxine-dependent epilepsy. *Neuropediatrics* 36: 200–205.
- Plecko, B., K. Paul, E. Paschke, S. Stoeckler-Ipsiroglu, E. Struys *et al.*, 2007 Biochemical and molecular characterization of 18 patients with pyridoxine-dependent epilepsy and mutations of the antiquitin (ALDH7A1) gene. *Hum. Mutat.* 28: 19–26.
- Sander, J. D., M. L. Maeder, D. Reyon, D. F. Voytas, J. K. Joung *et al.*, 2010 ZiFiT (Zinc Finger Targeter): an updated zinc finger engineering tool. *Nucleic Acids Res.* 38: W462–W468.
- Schmitt, B., M. Baumgartner, P. B. Mills, P. T. Clayton, C. Jakobs *et al.*, 2010 Seizures and paroxysmal events: symptoms pointing to the diagnosis of pyridoxine-dependent epilepsy and pyridoxine phosphate oxidase deficiency. *Dev. Med. Child Neurol.* 52: e133–e142.
- Sourbron, J., H. Schneider, A. Kecskes, Y. Liu, E. M. Buening *et al.*, 2016 Serotonergic modulation as effective treatment for Dravet syndrome in a zebrafish mutant model. *ACS Chem. Neurosci.* 7: 588–598.
- Srivastava, A., K. Hamre, J. Stoss, R. Chakrabarti, and S. K. Tonheim, 2006 Protein content and amino acid composition of the live feed rotifer (*Brachionus plicatilis*): with emphasis on the water soluble fraction. *Aquaculture* 254: 534–543.
- Stockler, S., B. Plecko, S. M. Gospe, M. Coulter-Mackie, M. Connolly *et al.*, 2011 Pyridoxine dependent epilepsy and antiquitin deficiency. Clinical and molecular characteristics and recommendations for diagnosis, treatment and follow-up. *Mol. Genet. Metab.* 104: 48–60.
- Struys, E. A., and C. Jakobs, 2010 Metabolism of lysine in alpha-amino adipic semialdehyde dehydrogenase-deficient fibroblasts: evidence for an alternative pathway of pipecolic acid formation. *FEBS Lett.* 584: 181–186.
- Struys, E. A., L. A. Bok, D. Emal, S. Houterman, M. A. Willemsen *et al.*, 2012a The measurement of urinary Δ^1 -piperidine-6-carboxylate, the alter ego of α -amino adipic semialdehyde, in Antiquitin deficiency. *J. Inher. Metab. Dis.* 35: 909–916.
- Struys, E. A., B. Nota, A. Bakkali, S. Al Shahwan, G. S. Salomons *et al.*, 2012b Pyridoxine-dependent epilepsy with elevated urinary α -amino adipic semialdehyde in molybdenum cofactor deficiency. *Pediatrics* 130: e1716–e1719.
- Teng, Y., X. Xie, S. Walker, G. Rempala, D. J. Kozlowski *et al.*, 2010 Knockdown of zebrafish *Lgi1a* results in abnormal development, brain defects and a seizure-like behavioral phenotype. *Hum. Mol. Genet.* 19: 4409–4420.
- Teng, Y., X. Xie, S. Walker, M. Saxena, D. J. Kozlowski *et al.*, 2011 Loss of zebrafish *Igllb* leads to hydrocephalus and sensitization to pentylenetetrazol induced seizure-like behavior. *PLoS One* 6: e24596.
- Tóth, K., and Z. Maglóczy, 2014 The vulnerability of calretinin-containing hippocampal interneurons to temporal lobe epilepsy. *Front. Neuroanat.* 8: 1–12.
- Tóth, K., L. Eross, J. Vajda, P. Halász, T. F. Freund *et al.*, 2010 Loss and reorganization of calretinin-containing interneurons in the epileptic human hippocampus. *PLoS One* 5: e12577.
- Treiman, D. M., 2001 GABAergic mechanisms in epilepsy. *Epilepsia* 42: 8–12.
- van der Ham, M., M. Albersen, T. J. de Koning, G. Visser, A. Middendorp *et al.*, 2012 Quantification of vitamin B6 vitamers in human cerebrospinal fluid by ultra performance liquid chromatography-tandem mass spectrometry. *Anal. Chim. Acta* 712: 108–114.
- van Karnebeek, C. D. M., and S. Jaggamantri, 2015 Current treatment and management of pyridoxine-dependent epilepsy. *Curr. Treat. Options Neurol.* 17: 335.
- van Karnebeek, C. D. M., H. Hartmann, S. Jaggamantri, L. A. Bok, B. Cheng *et al.*, 2012 Lysine restricted diet for pyridoxine-dependent epilepsy: first evidence and future trials. *Mol. Genet. Metab.* 107: 335–344.
- van Karnebeek, C. D. M., S. A. Tiebout, J. Niermeijer, B. T. Poll-The, A. Ghani *et al.*, 2016 Pyridoxine-dependent epilepsy: an expanding clinical spectrum. *Pediatr. Neurol.* 59: 6–12.
- Waterval, W. A. H., J. L. J. M. Scheijen, M. M. J. C. Ortman-Ploemen, C. D. Habets-van der Poel, and J. Bierau, 2009 Quantitative UPLC-MS/MS analysis of underivatized amino acids in body fluids is a reliable tool for the diagnosis and follow-up of patients with inborn errors of metabolism. *Clin. Chim. Acta* 407: 36–42.
- Waymire, K. G., J. D. Mahuren, J. M. Jaje, T. R. Guilarte, S. P. Coburn *et al.*, 1995 Mice lacking tissue non-specific alkaline phosphatase die from seizures due to defective metabolism of vitamin B-6. *Nat. Genet.* 11: 45–51.
- Weiss, M. J., D. E. Cole, K. Ray, M. P. Whyte, M. A. Lafferty *et al.*, 1988 A missense mutation in the human liver/bone/kidney alkaline phosphatase gene causing a lethal form of hypophosphatasia. *Proc. Natl. Acad. Sci. USA* 85: 7666–7669.
- Westerfield, M., 2000 *The Zebrafish Book. A guide for the Laboratory use of Zebrafish (Danio Rerio)*. University of Oregon Press, Eugene, OR.
- Wilkinson, R. N., S. Elworthy, P. W. Ingham, and F. J. M. van Eeden, 2013 A method for high-throughput PCR-based genotyping of larval zebrafish tail biopsies. *Biotechniques* 55: 314–316.
- Xia, J., and D. S. Wishart, 2002 Using MetaboAnalyst 3.0 for comprehensive metabolomics data analysis. *Curr. Protoc. Bioinformatics* 55: 14.10.1–14.10.91.
- Xia, J., I. V. Sinelnikov, B. Han, and D. S. Wishart, 2015 MetaboAnalyst 3.0—making metabolomics more meaningful. *Nucleic Acids Res.* 43: W251–W257.
- Yang, Z., X. Yang, Y. Wu, J. Wang, Y. Zhang *et al.*, 2014 Clinical diagnosis, treatment, and ALDH7A1 mutations in pyridoxine-dependent epilepsy in three Chinese infants. *PLoS One* 9: e92803.
- Zhang, Y., A. Kecskés, D. Copmans, M. Langlois, A. D. Crawford *et al.*, 2015 Pharmacological characterization of an antisense knockdown zebrafish model of Dravet syndrome: inhibition of epileptic seizures by the serotonin agonist fenfluramine. *PLoS One* 10: e0125898.
- Zhu, X., Y. Xu, S. Yu, L. Lu, M. Ding *et al.*, 2014 An efficient genotyping method for genome-modified animals and human cells generated with CRISPR/Cas9 system. *Sci. Rep.* 4: 6420.

Communicating editor: D. Greenstein